

# POLITECNICO DI TORINO

Master's Course in Biomedical Engineering

*Department of Mechanical and Aerospace Engineering*



Master Degree Thesis in Biomedical Engineering

## **Immune-Derived Exosomes Mimetics (IDEM) as an innovative, versatile and biomimetic nanoparticle system for cancer treatment**

***Supervisor:***

*Prof. Gianluca Ciardelli*

***External Supervisor:***

*Prof. Bruna Corradetti*

*Houston Methodist Research Institute*

*Department of Nanomedicine - Houston, Texas (USA)*

***Candidate:***

*Irene Pierini*

*Academic year 2019-2020*

*To Mari,*  
*my αγάπη*

# CONTENTS

|  |      |    |
|--|------|----|
| <b>1. Preface</b> .....  | Page | 6  |
| <b>2. Abstract</b> .....                                       | Page | 7  |
| <b>3. Introduction</b> .....                                   | Page | 9  |
| 3.1. What is a tumor   | “    | 9  |
| 3.2. Tumor therapies   | “    | 10 |
| 3.3. Exosomes  | “    | 11 |
| 3.3.1. Biogenesis, characteristics and functions               | “    | 11 |
| 3.3.2. Potential applications of exosomes                      | “    | 13 |
| 3.3.3. Exosomes and tumor                                      | “    | 14 |
| 3.3.4. Comparison between exosomes and other nanoparticles     | “    | 15 |
| 3.3.5. Clinical limits of exosomes                             | “    | 16 |
| 3.3.6. Laboratory production of engineered exosomes            | “    | 16 |
| 3.4. Immune-Derived Exosomes Mimetics (IDEM)                   | “    | 17 |
| 3.4.1. The advantages of using IDEM                            | “    | 17 |
| 3.4.2. The use of exosomes to treat ovarian cancer             | “    | 18 |
| 3.5. The aim of the study                                      | “    | 19 |
| <b>4. Materials and Methods</b> .....                          | Page | 20 |
| 4.1. Cell lines and media                                      | “    | 20 |
| 4.1.1. Thp-1, monocytic cell line                              | “    | 20 |
| 4.1.2. Skov3, ovarian cancer cell line                         | “    | 20 |
| 4.2. Natural exosomes (EXO) extraction                         | “    | 21 |
| 4.3. Synthesis of IDEM   | “    | 22 |
| 4.4. Dimensional characterization and concentration assessment | “    | 23 |
| 4.4.1. Nanoparticle Tracking analysis (NTA-NANOSIGHT)          | “    | 23 |
| 4.4.1.1. Physical principles                                   | “    | 23 |
| 4.4.1.2. Protocol  | “    | 24 |
| 4.4.2. Scanning electron microscopy (SEM)                      | “    | 25 |
| 4.4.2.1. Physical principle                                    | “    | 25 |
| 4.4.2.2. Protocol  | “    | 26 |

|           |  |             |           |
|-----------|--|-------------|-----------|
| 4.5.      | Protein content characterization: western blot             | Page        | 27        |
| 4.5.1.    | Physical principles  | "           | 27        |
| 4.5.2.    | Protocol   | "           | 28        |
| 4.6.      | Flow cytometry   | "           | 31        |
| 4.6.1.    | Physical principles  | "           | 31        |
| 4.6.2.    | Protocols  | "           | 32        |
| 4.7.      | Test drug cytotoxicity and 2D cell viability assessment    | "           | 34        |
| 4.7.1.    | Physical principle   | "           | 34        |
| 4.7.2.    | Protocols  | "           | 34        |
| 4.8.      | Encapsulation efficiency (EE%)                             | "           | 36        |
| 4.9.      | Drug release (DR%)   | "           | 37        |
| 4.10.     | E-Sight  | "           | 39        |
| 4.10.1.   | Physical principle   | "           | 39        |
| 4.10.2.   | Protocol   | "           | 40        |
| 4.11.     | Confocal microscopy  | "           | 41        |
| 4.11.1.   | Physical principle   | "           | 41        |
| 4.11.2.   | Protocol   | "           | 42        |
| 4.12.     | 3D cultures and IDEM cytotoxicity                          | "           | 43        |
| 4.12.1.   | Physical principle   | "           | 43        |
| 4.12.2.   | Protocol   | "           | 44        |
| 4.13.     | Statistical analysis                                       | "           | 45        |
| <b>5.</b> | <b>Results and Discussion . . . . .</b>                    | <b>Page</b> | <b>46</b> |
| 5.1.      | Dimensional characterization and concentration assessment  | "           | 46        |
| 5.1.1.    | Nanoparticle Tracking Analysis                             | "           | 46        |
| 5.1.2.    | Scanning Electron Microscopy (SEM)                         | "           | 48        |
| 5.2.      | Protein content characterization                           | "           | 49        |
| 5.2.1.    | Western blot   | "           | 50        |
| 5.2.2.    | Optimization of western blot for exosomes characterization | "           | 51        |
| 5.2.3.    | Flow cytometry   | "           | 51        |
| 5.3.      | Test drug cytotoxicity                                     | "           | 52        |
| 5.4.      | Encapsulation efficiency (EE%)                             | "           | 53        |
| 5.5.      | Drug release (DR%)   | "           | 53        |
| 5.6.      | 2D cultures and IDEM cytotoxicity                          | "           | 54        |
| 5.6.1.    | Alamar blue  | "           | 54        |
| 5.6.2.    | E-Sight  | "           | 56        |
| 5.7.      | Cellular uptake  | "           | 57        |
| 5.7.1.    | Confocal microscopy  | "           | 57        |
| 5.7.2.    | Flow cytometry   | "           | 58        |
| 5.8.      | 3D cultures and IDEM cytotoxicity                          | "           | 60        |

|  |      |    |
|--|------|----|
| <b>6. Conclusions</b> .....  | Page | 62 |
| <b>7. Other skills acquired during my experience at Corradetti Lab</b> ..... | Page | 64 |
| 7.1. Animal testing  | “    | 64 |
| 7.2. Rendering of exosomes and 3D printing                                   | “    | 66 |
| <b>8. Acknowledgments</b> .....  | Page | 68 |
| <b>9. Bibliography</b> .....   | Page | 72 |

# 1. Preface

Houston Methodist (HM) is one of the hospitals located in the Texas Medical Center (TMC) of Houston, Texas (USA). HM is a leader in Healthcare, it's the first Hospital in Texas for patient care and among the top 20 hospitals in United States. The motto and philosophy of HM is the ICARE value (integrity, compassion, accountability, respect and excellence) and all the workers do their best to make it practice, from healthcare to spiritual care, research and internal organization. Houston Methodist Research Institute (HMRI) is also located at TMC and it's the institution delegated to research in medical field, from cancer to other diffused diseases and other fundamental aspects of healthcare, in order to develop and increase the level of cures in all the aspects. The Department of Nanomedicine performs a fundamental part of research at HMRI and Professor Bruna Corradetti is one of the Principal Investigator (PI) that are involved in developing innovative immunomodulatory approaches for the treatment of chronic diseases, including cancer. HMRI and Nanomedicine Department have as an objective the collaboration and partnership with hospitals, patients, enterprises and workers, without forgetting the ICARE values. This environment is the key for success and for the progress of the present to a healthier world.



*Logo of Houston Methodist Hospital*

## 2. Abstract

Exosomes are extracellular nanovesicles naturally produced by cells through the invagination of their membrane and are involved in cell-to-cell communication and content exchange. They have specific characteristics in terms of dimension, structure and surface proteins expression and they can be loaded with drugs for specific cell targeting. These features allow them to avoid the induction of an immune response and to take advantage of the enhanced permeability and retention effect, which is required for accumulation of drug in a specific area. They are versatile nanoparticles, with the potential to be engineered or loaded with specific drugs to achieve an enhanced immune system activation against cancer cells, a more efficient tumor cell targeting, with the consequent reduction of the side effects induced by the drug. Their lipid structure protects the drug or biological compound loaded and allows for the prolonged maintenance of its bioactivity. However, their applicability in clinical settings is currently limited by the low yield, scarce scalability, poor batch-to-batch reproducibility and time-consuming synthesis.

The purpose of this thesis is to develop a strategy to obtain biomimetic nanoparticles with the potential to be used as carriers of chemotherapeutics for cancer treatment. These nanoparticles were defined as Immune Derived Exosomes Mimetics (IDEM) as they were synthesized by sequentially forcing immune cells (monocytic cell line, THP1) through 8 $\mu$ m and 10 $\mu$ m dimensional filters and applying serial cycles of centrifugation.

IDEM were characterized in comparison with naturally derived exosomes (EXO) extracted from the culture media of the same number of cells through standard protocols. IDEM and EXO were analyzed by western blot and flow cytometry for protein expression, whereas Scanning Electron Microscope (SEM) and Nanoparticle Tracking analysis (NTA) were used for their morphological characterization and to determine particle concentration, respectively. The IDEM approach provided a greater number of nanoparticles compared to natural exosomes ( $9.42 \times 10^9 \pm 2.31 \times 10^9$  exosomes/mL and  $2.34 \times 10^{10} \pm 7.91 \times 10^9$  IDEM/mL). Although with a slightly larger diameter compared to EXO ( $177.08 \pm 19.64$  nm versus  $112.44 \pm 14.59$  nm, respectively) IDEM size fell within the exosomal dimensional range. We also confirmed the

similarity of the two formulations in terms of exosomal protein content (i.e. tetraspanins CD63, CD81, ALIX and TSG101). As a proof of concept, EXO and IDEM were loaded with Doxorubicin and the encapsulation efficiency (EE%) and drug release profile studies were performed. IDEM showed an increase in EE% and a similar drug release profile compared to EXO, presenting a burst release of 55% of the encapsulated drug in the first 12 hours. The cytotoxic effect of different doses of doxorubicin-loaded (DOX-loaded) IDEM and EXO was tested on the human ovarian cancer cell line SKOV3 and monitored over a 96-hour period. The Alamar Blue assay and the measurement of impedance of adherent cells executed through the xCelligence Sight were used for cell viability assessment. We also verified the drug uptake by cells with flow cytometry and confocal microscopy. Data obtained revealed that the lower concentration (1µg/mL) of IDEM and EXO compared to free Doxorubicin (10µg/mL) was sufficient to kill cancer cells. Lastly, the cytotoxicity of 3µg/mL dose doxorubicin-loaded IDEM and EXO was tested in 3D experiment by monitoring SKOV3 spheroids viability for 96 hours. Data showed that also in a 3D model, IDEM and EXO with lower drug concentration are more cytotoxic than free Doxorubicin.

With this work we can conclude that IDEM hold potential for innovative cancer treatments as they couple the advantages of natural exosomes with the higher reproducibility and production yields.

## 3. Introduction

### 3.1. What is a tumor

Cancer is an umbrella-word that includes over a hundred different diseases that have in common the uncontrolled division of cells of the body. It can affect any type of tissue from the skin to the neurons with different pathways and development. However, they all have a common starting point. Indeed, a cell becomes cancerous whenever the inhibitors of cell division stop working because of a mutation for example, so that cells are able to proliferate uncontrollably. Also, their daughter cells will present the same mutation, leading to increase cancer cell proliferation and the formation of a tumor mass. This mass can stay *in situ* and remain a primary tumor or invade other tissues through the blood by the extravasation and spreading of tumor cell subpopulations, which is called metastasis and leads to a malignant or invasive tumor. The tumor starts to be lethal whenever it absorbs all the survival nutrients from the hosting-body [1]. In **Figure 3.1** [2] a simple scheme of the said above process is shown.

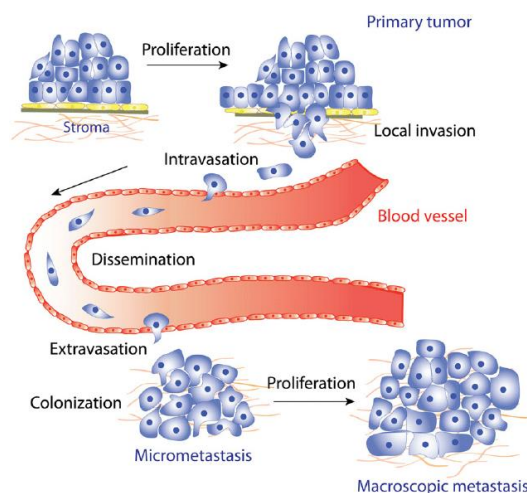


Figure 3.1: behavior and development of cancer cells, from a stroma to a metastasis

There are many types of tumor and they can be divided in base of the affected tissues (i.e. Adenoma from epithelial tissue, Fibroma from fibrous or connective tissue, Hemangiomas from blood cells and Lipoma from adipose cells) [3].

Tumors can also be defined as “hot” and “cold”. Hot tumors show signs of inflammation and immune activation, meaning that it’s already penetrated by leukocytes (i.e. T-cells, natural killer cells or macrophages) and has been recognized as a threat by the immune system. The latter, on the contrary, presents low levels of immune cells infiltration and hence of immune activation, making it hard to target with the current immunotherapies [4].

### 3.2. Tumor therapies

Based on the type and stage of tumor, different therapies can be applied. Generally, if the tumor is *in situ*, surgical removal is used. The surgery becomes more challenging if the tumor is metastatic. Chemotherapy is used to treat all stages of cancer, for example it can be used to shrink a tumor before radiation therapy or surgery (called neoadjuvant chemotherapy); to destroy any remaining cancer cells after a treatment such as surgery, radiation, immunotherapy or hormone therapy; to make another treatment more effective; to destroy any cancer recurring or metastasis, like for example in ovarian cancer treatment [5]. Chemotherapy and radiotherapy are the most common way to treat cancer, but in recent years also immunotherapy against hot tumors and hormone therapy are becoming promising cures [6]. Unfortunately, cold tumors are currently challenging in terms of cure.

New approaches are getting more and more used such as targeted therapy by using nanoparticles as carrier of cancer treatment [7]. Targeted therapy uses antibodies, genes, proteins or characteristics of cancer tissues to directly recognize cancer cells and to specifically kill them without damaging healthy cells. Nanocarrier made of polymer, metal or lipids loaded with a drug are also another targeted therapy method. It is composed by two main categories: passive and active targeting. The first one exploits the enhance permeability and retention (EPR) effect through which the nanoparticles reach cancer cells by passing through the leaking and highly permeable tumor blood vessels, which are weaker and more permeable than the healthy ones [8]. Also, the poor lymphatic drainage in tumors contributes to the nanoparticle retention. Both

these actions increase the efficacy of anti-cancer treatment [6]. The second targeting way is the active one, in which the nanoparticles is functionalized with antibodies, surface proteins, receptors in order to specifically target the tumor cell. In **Figure 3.2** [9], the mechanism of action of active and passive targeting strategies is provided. Other two therapies for cancer treatment are stem cell transplant and precision medicine (based on study of genetic studies to develop select treatments).

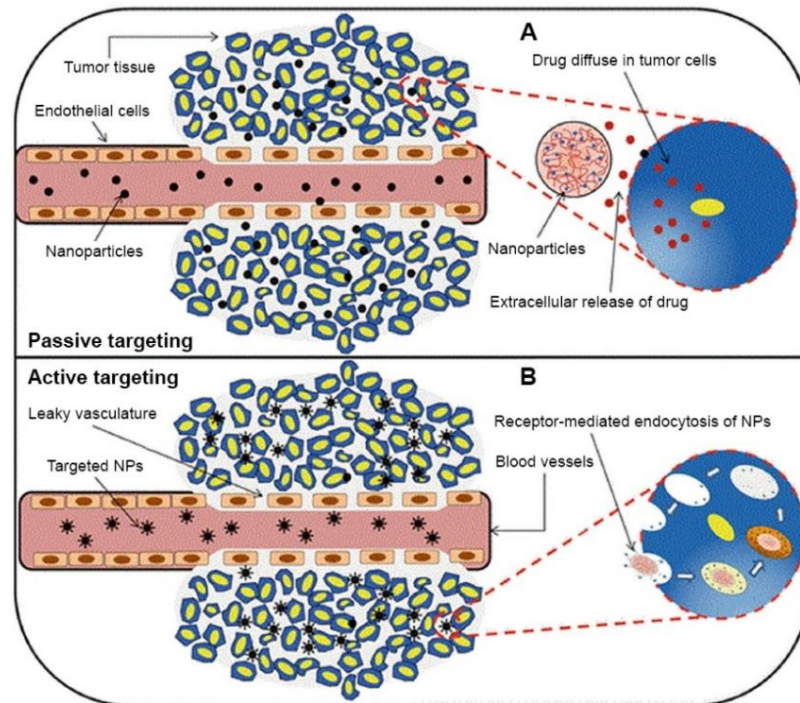


Figure 3.2: Mechanism of action of passive and active targeting for cancer treatment

### 3.3. Exosomes

#### 3.3.1. Biogenesis, characteristics and functions

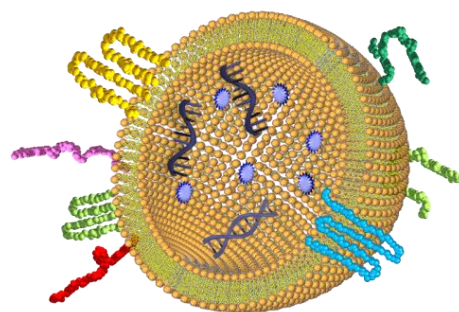


Figure 3.3.1: Simplified image of an exosome. It's possible to see the double phospholipid layer, the transmembrane proteins such as tetraspanins, the internal contents (DNA, RNA, drugs, peptides, cell debris)

Exosomes are extracellular nanovesicles naturally secreted by any type of cells (**Figure 3.3.1**). They were discovered in the late 1980s and they were initially considered a waste product of cell metabolism or cell damages, with no significant influence on neighboring cells [10]. Only in the last few years exosomes started to be studied for their content in terms of lipids, proteins, DNA, RNA and for their relation with metabolism and pathologies, since they are involved in cell-to-cell communication. They are constitutively generated from late endosomes, which are formed by inward budding of the cell membrane (**Figure 3.3.1.1** [11]). During this process, certain membrane proteins are incorporated into the nanovesicle membrane, while the cytosolic components are engulfed and enclosed within it, creating an early-endosome [12]. Tumor susceptible gene 101 (TSG101) and ALG-2-interacting Protein X (ALIX) proteins are involved in this formation step. Another pattern of formation of exosomes involves the tetraspanins CD63 and CD81 (transmembrane proteins, their name comes from the fact that they go through the cell membrane four times). The multi-vesicular body (MVB) that derives from this process merges with the cellular membrane and releases the exosomes outside the cell. Exosomes contain various components such as mRNA, enzymes, actin and other cytoskeletal proteins, DNA, miRNA and other nucleic species [13]. Markers such as ALIX, TSG101 and tetraspanins CD9, CD81, CD63 are commonly used as exosomes markers. Exosomes membrane is made of a double phospholipidic layer, with a diameter of 30-150 nm. Its main function is mediating intercellular communication by transferring functional substances inside them from once cell to the others, locally and distantly, in physiological and pathological status [14], which make them an important protagonist in possible efficient communication link for cancer treatment.

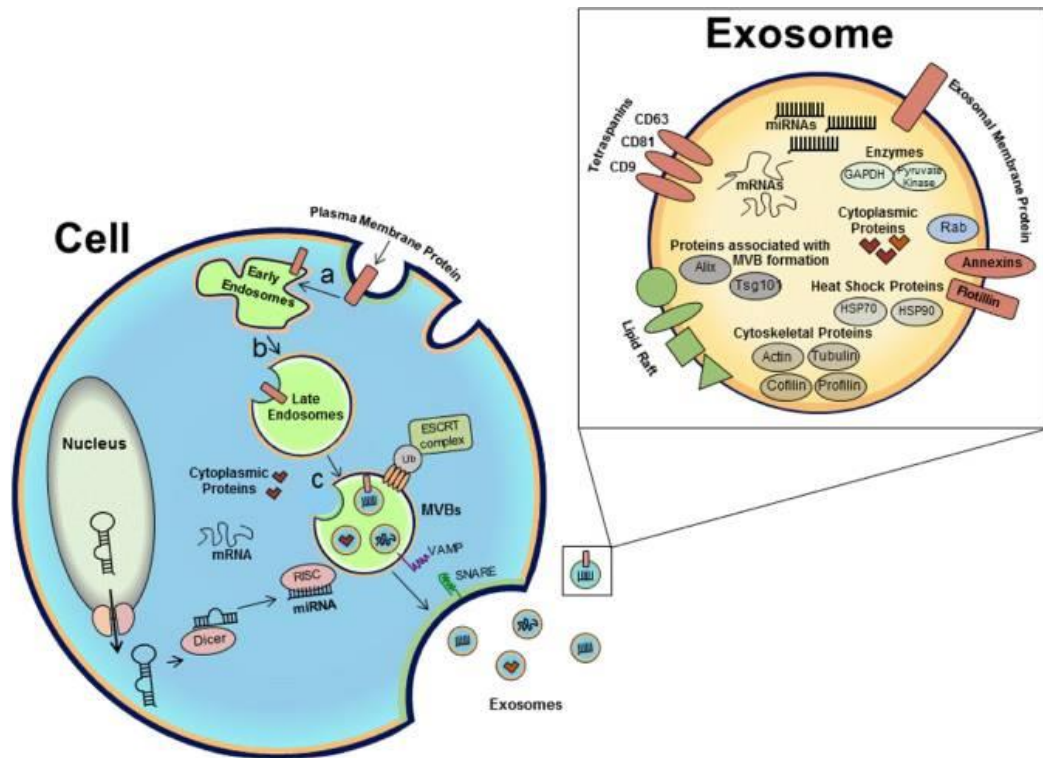


Figure 3.3.1.1: Formation of an exosome from a cell and main characteristics.

### 3.3.2. Potential applications of exosomes

Exosomes are a good ally for many treatments in the biomedical field as shown in **Figure 3.3.2**. In fact, they can be used as drug delivery vessels or as fluorochrome or contrast agent carrier in many fields such as oncology, cardiovascular, neurology. They can also be used as biomarkers for the early detection of a pathology since their content is strictly correlated to the cell status and health. They can be used as genomic carriers for genetic modifications, they can enhance inflammatory response like it's done in immunotherapy or in chronic wound healing, osteoarthritis and other articular diseases. They are very small, so they can penetrate many barriers such as the Blood Brain Barrier (BBB) and Blood Cerebrospinal Fluid Barrier (CSF) [15], two big obstacles for many current drugs. Exosomes can also have a role in diabetes mellitus development and treatment since they are one of the main communicators between hepatic cells. Lastly, they can be employed for regenerative medicine [16]. Their main positive aspect of using exosomes in clinical treatment is that they are not recognized as foreign compounds as it happens with cells from

donors [17], other chemical-biological compounds or implanted devices. The inflammatory response is induced only if exosomes are made to enhance it. Also, cell injections have high risk of degeneration in tumor [18].

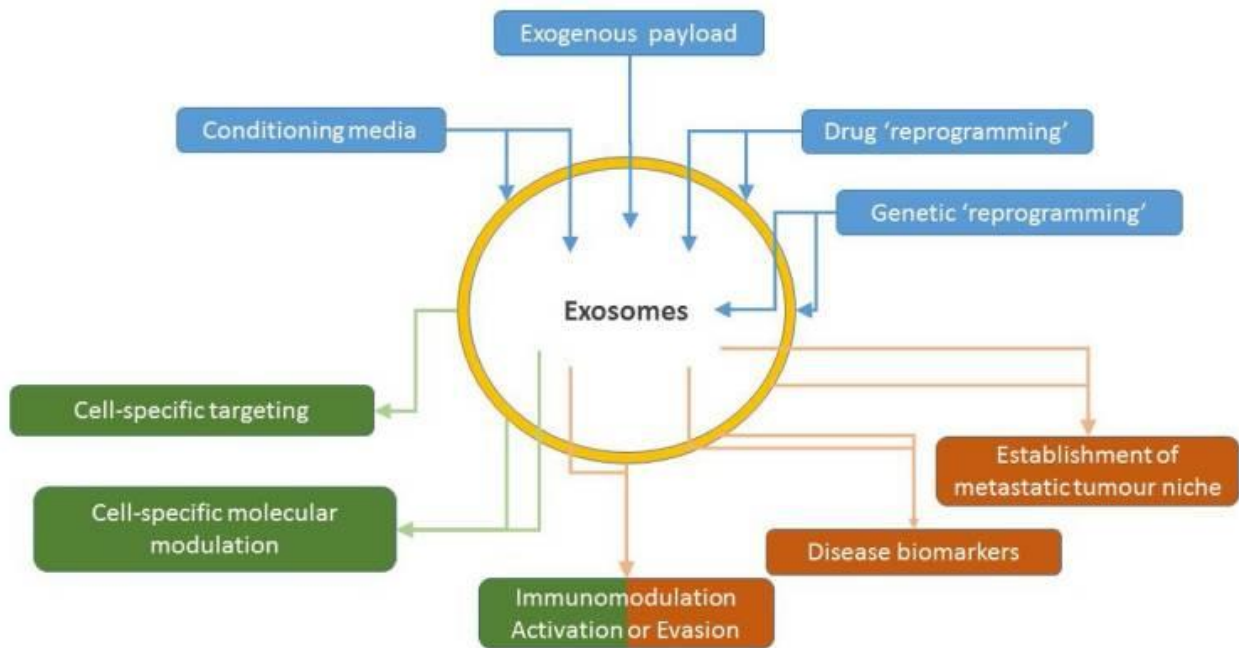


Figure 3.3.2: brain storming of all the possible applications of exosomes as therapeutic agent

### 3.3.3. Exosomes and tumor

Exosomes are involved in angiogenesis, invasiveness, immune resistance and metastasis of cancer cells [19] [20]. This means that they could represent a means of communication with the tumor in order to effectively treat it. In fact, exosomes can be used as regulators of cancer progression by modulating the immune system like a vaccine, decreasing angiogenesis, reprogramming stromal cells. They can also tune proliferation, drug resistance, modify the micro-environment. Furthermore, exosomes can be loaded with a chemotherapeutic compound in order to decrease side effects and increase efficiency of chemotherapy, they can interfere in metastasis development by inhibiting cancer cell-to-cancer cell communication. Lastly, exosomes can be loaded also with genetic compounds in order to modify the genetic expression of a cancer cells and heal it or kill it [21].

### 3.3.4. Comparison between exosomes and other nanoparticles

Several nanoparticles are already FDA approved such as DOXIL (**Figure 3.3.4 a** [22]), ONIVYDE and ABRAXANE (**Figure 3.3.4 c** [23]), which are lipid or polymeric nanoparticles with an internal core where the drug or the biological compound is encapsulated in order to avoid degradation from biological liquids and to efficiently target it to specific pathological areas. They are also functionalized on the surface to obtain the specific targeting. However, cancer cells quickly adapt to the nanoparticle treatment, which leads to modification of surface expression, and consequentially the cure becomes ineffective. In **Figure 3.3.4 b** [24], the most famous and studied nanoparticles for clinical application are shown. Despite all of them are good current way of disease treatment and diagnosis, they can activate immune response, they can be really expensive in production, they have low half-life, or they can be dangerous for the organism if not used properly [25].

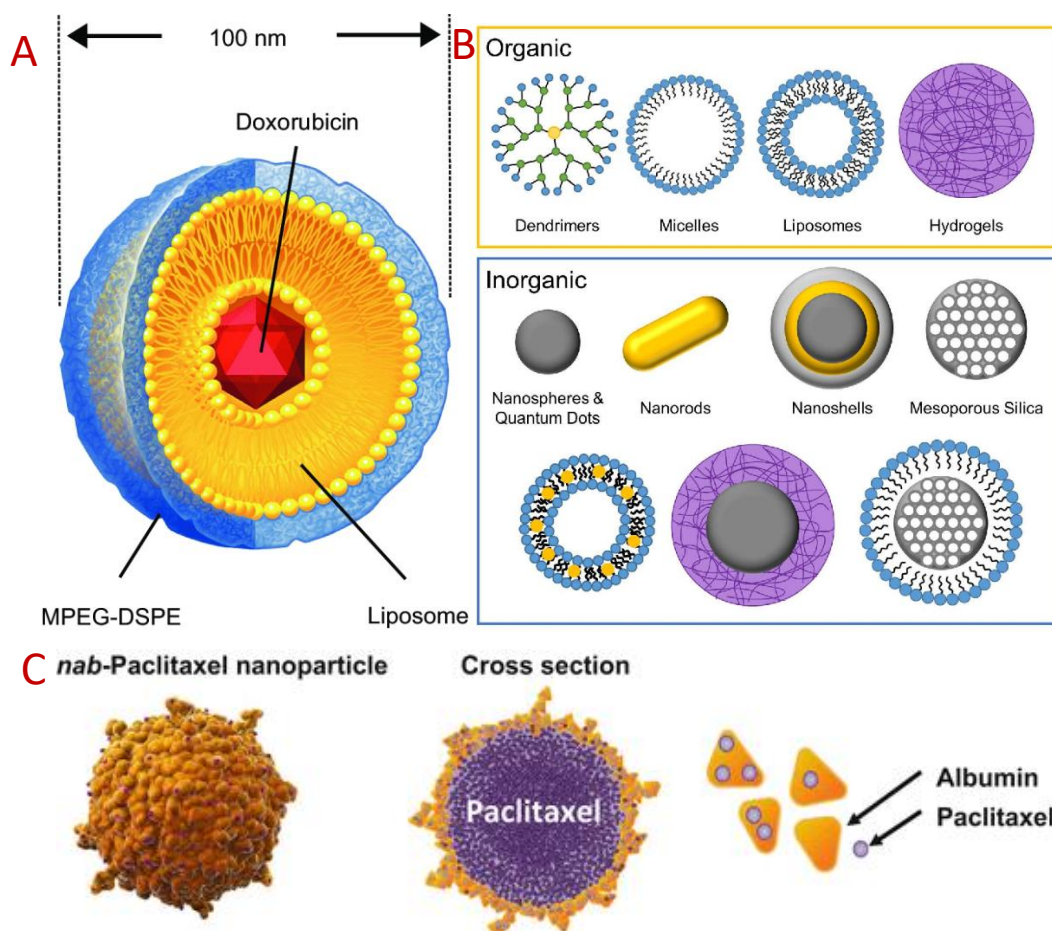


Figure 3.3.4: nanoparticles currently used or studied for clinical treatments or diagnostics. a) DOXIL structure; b) Organic and Inorganic nanoparticles; c) ABRAXANE structure

### 3.3.5. Clinical limits of exosomes

Exosomes are promising nanoparticles for new therapies, but their extraction yield strictly depends on the operator and on the extraction protocol, which means that their characteristics are not replicable and with low yield [26] [27]. This leads to a challenging large-scale production and consequently no clinical application due to the wide variability of the obtained sample and lack of standardization [28]. Protein content characterization is another aspect in which every exosomes extraction is different from the other starting from the same cell of origin [26]. Another big limitation is that purification from other nanovesicles (i.e. apoptotic debris, proteins aggregates and lipoprotein particles [29]) during extraction is not always well obtained, which means more contaminations, more variability, less success in their use for clinical purposes. Other problems are the difficult characterization of composition and contents of the vesicles that make difficult to predict in vivo activity; the abundant and diverse bioactive contents of vesicles that can unpredictably effects and not-wanted consequences such as immune response or cellular apoptosis or phenotypical modifications [30]. Lastly, lack of techniques or resolution for detailed visualization and studies make their characterization trickier and less reliable [31]. Thus, while modulation of expression, composition and contents of natural exosomes are studied, parallel efforts are being made in the development of biomimetic or synthetic drug-delivery platforms.

### 3.3.6. Laboratory production of engineered exosomes

The main method of exosome extraction and isolation is by ultracentrifugation or differential centrifugation. In particular, these methods alternate several centrifugation steps (in order to eliminate all the microparticles and dead cells) at increased spin velocity with purification of the sample such as filtration with smaller pores as soon as the protocol is moved forward [32]. Other methods include size exclusion chromatography, filtrations or sieving and immunological separation. In **Table 3.3.6** [33] a list of all the methods for exosome isolation are shown.

| Isolation methods               | Mechanism   | Advantages  | Disadvantages   |
|---------------------------------|---|---|---|
| Differential centrifugation     | The method consists of several centrifugation steps aiming to remove cells, large vesicles and debris and precipitate exosomes.   | Differential centrifugation is the standard and very common method used to isolate exosomes from biological fluids and media.   | The efficiency of the method is lower when viscous biological fluids such as plasma and serum are used for analysis.  |
| Density gradient centrifugation | This method combines ultracentrifugation with a sucrose, or iodixanol, density gradient.  | The method allows separation of the low-density exosomes from other vesicles, particles and contaminants.   | Very high sensitivity to the centrifugation time.   |
| Size exclusion chromatography   | Size-exclusion chromatography separates macromolecules on the base of their size. It applies a column packed with porous polymeric beads.                                   | The method allows the precise separation of large and small molecules and application of various solutions. Compared to centrifugation methods, the structure of exosomes isolated by shearing force. | The method requires a long running time, which limits applications of chromatographical isolation for processing multiple biological samples.   |
| Filtration                      | Ultrafiltration membranes are used to separate exosomes from proteins and other macromolecules. The exosomal population is concentrated on the membrane.                    | Filtration allows separation of small particles and soluble molecules from exosomes. During the process the exosomal population is concentrated by the filtration membrane.                           | Exosomes can adhere to the filtration membranes and become lost for the following analysis. Also, since the additional force is applied to pass the analyzed liquid through the membranes, the exosomes can potentially be deformed or damaged. |
| Polymer-based precipitation     | The technique includes mixing the biological fluid with polymer-containing precipitation solution, incubation step and centrifugation at low speed.                         | The advantages of precipitation include the mild effect on isolated exosomes and usage of neutral pH.   | Polymer-based precipitation methods co-isolate non-vesicular contaminants, including lipoproteins. Also, the presence of the polymer material may not be compatible with downstream analysis.   |
| Immunological separation        | Various immunological methods are applied. Magnetic beads bound to the specific antibodies are used to isolate exosomes. Also, ELISA-based separation method was developed. | The method allows isolation of all exosomes or selective subtypes of exosomes. Also, it may be applied for characterization and quantitation of exosomal proteins.                                    | The method is not applicable for large sample volumes. Also, the isolated vesicles may lose the functional activity.  |
| Isolation by sieving            | This technique isolates exosomes by sieving them via a membrane and performing filtration by pressure or electrophoresis.   | Relatively short separation time and gives high purity of isolated exosomes.  | Low recovery of isolated exosomes.  |

Table 3.3.6 Comparison of different methods of extraction of exosomes.

Regarding engineered laboratory synthesis of exosomes, synthetic exosome-mimics by cell extrusion or cell membrane-cloaked nanoparticles are the most commonly developed, they can be fabricated on a large-scale and provide novel platforms for drug delivery [34].

### 3.4. Immune-Derived Exosomes Mimetics (IDEM)

#### 3.4.1. The advantages of using IDEM

Immune-Derived Exosomes Mimetics (IDEM) are nanoparticles that are synthesized with the aim to mimic the shape, structure and protein expression of exosomes but using a faster, more reproducible and with higher yield method of production. In their synthesis procedure, cells are directly used as the nanoparticle source. In fact, they are disrupted by forcing their passage through

filters of different dimensions while under cycles of centrifugation. IDEM are similar to natural exosomes in protein content, shape and structure, so their nature is not compromised, but by synthesizing them, we can control their characteristics, tune them for our purposes and aim to a scalable production for clinical application in patients.

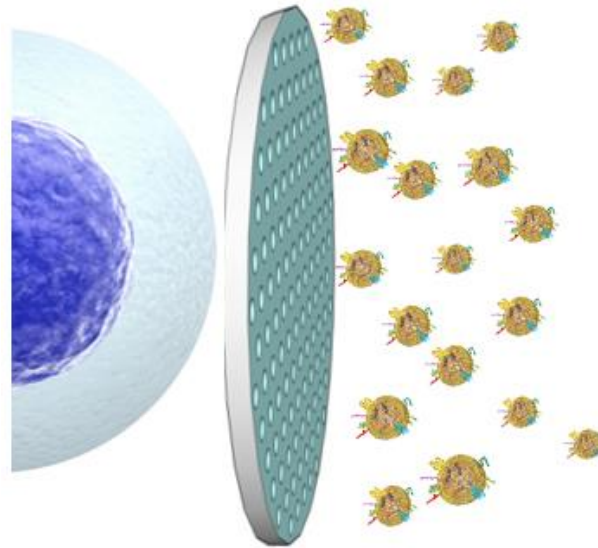


Figure 3.4.1: simplified view of how IDEM are cell-derived with a semi-synthetic protocol

### 3.4.2. The use of exosomes to treat ovarian cancer

Ovarian cancer is the fifth most common cause of cancer mortality in women because of lack of symptoms and it's characterized by the uncontrolled proliferation of ovary cells. In Italy is the 3% of all the tumor diagnosis, whereas in Europe it represents the 5% of all the female tumors [35]. There are many types of ovarian cancer, the epithelial is the most common one (90% of the cases [36]) and it involves the epithelial cells of ovaries. Symptoms of ovarian cancer are really difficult to interpret since they are really close to the ones of other pathologies, for example swollen abdomen, aerophagy, frequent need to urinate, pelvic cramps, inexplicable weight loss, pain during sexual intercourse [37]. Due to this underhand signal, ovarian cancer is really difficult to diagnose at early stage, so the tumor is already at stage III or IV at the moment of diagnosis and the survival rate is under 25%. Moreover, it is a cold tumor, so the immunotherapy is ineffective. Current treatments are surgical removal of the tumor or chemotherapy [38]. Another way of treatment is needed, that's why

exosomes can be used as an alternative to the above-mentioned methods. In fact, exosomes can be a specific, more effective and more efficient way to treat cancer (from immunotherapy [39] to drug-loading and administration, to diagnosis [40]) as mentioned before, but they also have the limits described in Chapter 3.3.5. In this work, it will be proved that IDEM have the same characteristics of exosomes regarding dimensions, shape and protein content, they are well recognized by the cell since they are rapidly incorporated by the cells, they are cytotoxic if chemotherapeutic-drug-loaded, but they have higher yield and less time-consuming synthesis, they are scalable for future pharmaceutical production and clinical application, they are versatile since they potentially could be produced for different cancers, from different cell sources, and they are batch-to-batch more reproducible than exosomes.

### **3.5. The aim of the study**

The objective of this thesis was to develop a strategy to obtain IDEM, a versatile and smart nanoparticle platform bioinspired by exosomes with the potential to be used as carriers of chemotherapeutics for cancer treatment. The nanoparticles were synthesized and characterized in shape, concentration and protein content, and then loaded with a chemotherapeutic drug and administered to ovarian cancer cells to study their cytotoxic potential. Throughout the entire study, natural exosomes were compared to IDEM in order to assess any differences or advantages when employing the semi-synthetic approach.

## 4. Materials and Methods

### 4.1. Cell lines and media

All cells were maintained in culture at 37°C, at humidified atmosphere and 5% CO<sub>2</sub>. Before their usage, all medias were heated at 37°C in a water bath and filtered through 0.22µm sterile PES syringe filters (Biopioneer).

#### 4.1.1. Thp-1, monocytic cell line

Human monocytic cell line THP-1 was provided by ATCC. THP-1 were maintained in culture with a density of 300,000-500,000 cells/mL in T75 flask (Nunc EasYFlask- Thermo Fisher Scientific) vertically positioned. When the cell density reached confluency, the cell suspension was centrifuged in a falcon tube at 300xg for 5 minutes. Cell media was then removed and the cell pellet was resuspended in fresh media.

Cell culture medium RPMI-1640 with L-glutamine (Invitrogen) was provided by American Type Culture Collection (ATCC). 10% Fetal Bovine Serum (FBS-Gibco) and 1% of Antibiotic-Antimycotic (A/A-Gibco) were added to empty medium.

For exosome extraction protocol, RPMI-1640 medium with L-glutamine (Invitrogen) with 10% exosome-depleted Fetal Bovine Serum (FBS-Gibco) and 1% of Antibiotic-Antimycotic (A/A-Gibco) was used. This media will be defined as Exo-free media from now on.

#### 4.1.2. Skov3, ovarian cancer cell line

Ovarian cystadenocarcinoma cell line SKOV3 was purchased from ATCC. SKOV3 were maintained in culture in T75 flask until reaching 80-90% of covered surface (confluence). To subculture them, cell culture media was aspirated and cells were washed in 10mL of Phosphate Buffer Saline pH 7.2 (PBS-Gibco-ThermoFisher Scientific). Cells were detached with 2.5mL of Trypsin-EDTA (SIGMA) for 5 minutes, that was then neutralized with 7.5mL of fresh media. Cell suspension

was then centrifuged in a falcon tube at 1200rpm for 5 minutes. Cell media was then removed and the cell pellet was resuspended in fresh media.

Cell culture media McCoy (Gibco) was purchased by Thermo Fisher Scientific. 10% Fetal Bovine Serum (FBS-Gibco) and 1% of Antibiotic-Antimycotic (A/A-Gibco) were added to empty medium.

## 4.2. Natural exosomes (EXO) extraction

This protocol was optimized by Corradetti Lab. 8.5 million THP1 cells were seeded in 13mL exo-free RPMI-1640 medium and left overnight. The following day, cells were centrifuged at 500xg for 5 minutes at room temperature to pellet cells. Without disturbing cell pellet, media was transferred to clean tube and centrifuged at 2000xg for 30 minutes at room temperature to pellet any remaining debris. The supernatant was then filtered through 0.22 $\mu$ m PES membrane syringe filter (Biopioneer) and then added to a 15mL 10 kDa Amicon ultra centrifugal filter (Millipore sigma) to concentrate the solution with a 4000xg centrifugation step of 15 minutes at room temperature. The concentrate was transferred to clean 1.5mL Eppendorf tube. Total exosome isolation reagent (from cell culture media, Invitrogen-Thermo Fisher Scientific) was added in the amount of half of the volume of suspension recovered, the solution was mixed by vortexing at least 30 seconds and incubated overnight at 4°C. The next day, the sample was centrifuge at 10,000xg for 1 hour at 4°C. The supernatant was then discarded without disturbing the cell pellet, which was resuspended in 85 $\mu$ L of 0.22 $\mu$ m filtered PBS. The samples were stored at -80°C for downstream applications.

In **Figure 4.2**, a schematic workflow of the exosome extraction protocol is shown.

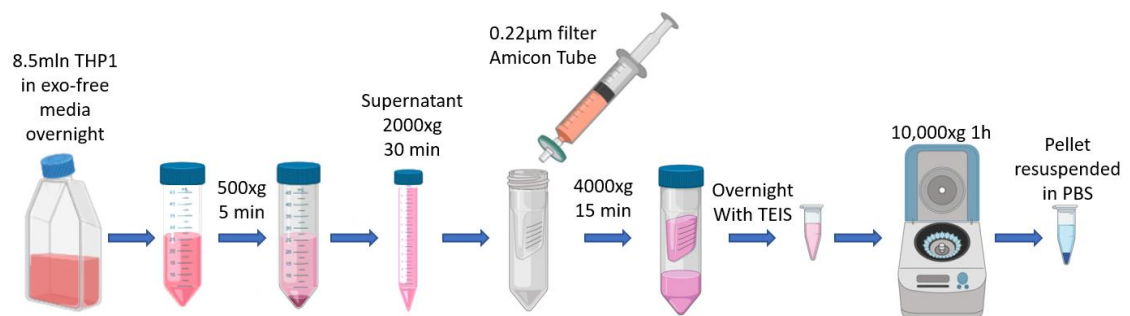


Figure 4.2: Schematic workflow of exosome extraction protocol.

### 4.3. Synthesis of IDEM

IDEM synthesis was performed optimizing an established protocol [41]. 8.5 million THP1 cells suspension were put in a falcon tube and centrifuged at 500xg for 5 minutes at room temperature. The supernatant was then removed, the cell pellet was washed with 1 mL of 0.22 $\mu$ m filtered PBS and then centrifuged at 500xg for 5 minutes at room temperature. The washing step was repeated twice. After the second wash, the supernatant was removed and the cell pellet was resuspended in 550 $\mu$ L of 0.22 $\mu$ m filtered PBS.

The suspension was then placed in a Pierce Spin Cups – 10 $\mu$ m Paper Filter (Thermo Fisher Scientific) and centrifuged at 14,000xg for 10 minutes at 4°C. The resulting pellet was then resuspended and re-added onto the same spin cup, repeating the same centrifuging step. Consequently, 8.0 $\mu$ m MCE Membrane filters (MF-Millipore) were cut in a circle shape and two were then placed with tweezers at the bottom of a new Pierce Spin Cup. Once the second centrifuge step was done, the pellet was resuspended in PBS and placed in the 8.0 $\mu$ m filter Pierce Spin Cup. The Spin cup was centrifuged at 14,000g for 10 minutes at 4°C, the supernatant was removed, and the cell pellet was resuspended in 85 $\mu$ L of 0.22 $\mu$ m filtered PBS.

An Exosome Spin Column (MW 3000-invitrogen-Thermo Fisher Scientific) was prepared following its protocol in order to remove any low molecular weight (MW  $\leq$  3000) admixtures from the exosome preparation such as salts, nucleotides, and short oligonucleotides. In particular, the column was tapped to settle the dry gel into the bottom of the column, it was hydrated with 650 $\mu$ L of 0.22 $\mu$ m filtered PBS, then it was vortexed, tapped to remove all the air bubble and let it rest for 5-15 minutes at room temperature. The spin column was then placed in a 2mL Collection Tube and it was centrifuged at 800xg for 2 minutes at room temperature. After having discarded the collection tube, the IDEM sample was immediately applied directly to the center of the column without touching the gel. The column was placed in a 1.5mL elution tube and centrifuged at 800xg for 2 minutes at room temperature, maintaining the same orientation of the gel of the previous centrifuge. Samples were stored at -80°C for downstream applications.

In **Figure 4.3** a block diagram of the protocol is shown.

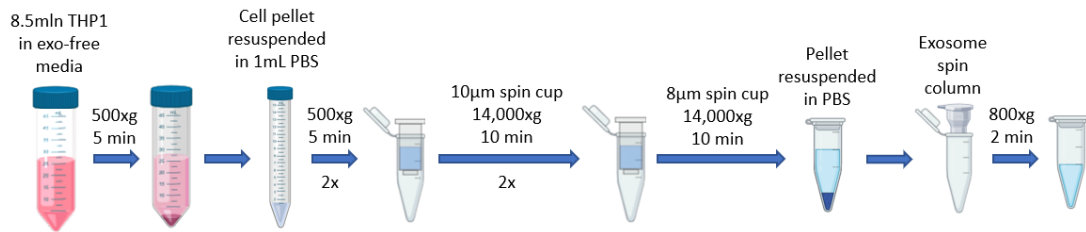


Figure 4.3: block diagram of IDEM synthesis protocol.

## 4.4. Dimensional characterization and concentration assessment

### 4.4.1. Nanoparticle Tracking Analysis (NTA-NANOSIGHT)

#### 4.4.1.1. Physical principles

NTA is a way to quantify and visualize suspensions of nanoparticles based on Brownian motion, typical of particles dispersed in liquid. In fact, by using the **Formula (a)**, NTA can relate the movement of the nanoparticle to its size [42].

$$(a) \quad \overline{(x, y)^2} = \frac{2k_B T}{3r_h \pi \eta}$$

Where  $\overline{(x, y)^2}$  is the mean squared speed of a particle at temperature  $T$ , in a medium of viscosity  $\eta$ , with a hydrodynamic radius of  $r_h$  and  $k_B$  is the Boltzmann constant. Thanks to this machine, we can measure size, concentration and fluorescence of nanoparticles in the range of 100 and 2500 nm and a concentration of  $10^7$ – $10^9$ /mL [43]. The machine is constituted by these main components:

- Microfluidic circuit in which the sample is injected by a syringe pump;
- Laser beam that illuminates the circuit in a chamber protected by light;
- Camera, it films the suspension that passes through the circuit;
- Computer with software for data processing.

A block scheme with all the components mentioned above is shown in **Figure 4.4.1.1 a** [44]. While the suspension passes through the microfluidic circuit, the nanoparticles in it interfere with the laser beam. The scattered light is then recorded with a camera perpendicular to the circuit. Every event will be

recorded and analyzed in post-processing. With the software it's possible to determine the camera level (brightness of the beam), set a flow rate, create scripts for data processing (number of videos, speed of the flow, interval between measurements etc.) and making post-processing analysis (threshold setting). NS300 (**Figure 4.4.1.1 b** [45]) is the machine that was used for measurement.

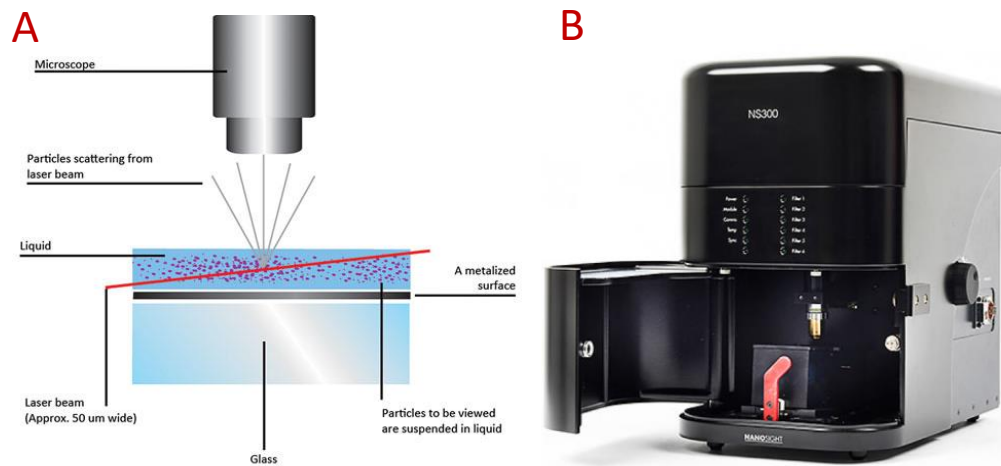


Figure 4.4.1.1: NTA characteristics, A) main components and B) model used in Corradetti Lab.

#### 4.4.1.2. Protocol

All the samples were constituted of 1mL or 500 $\mu$ L of solution with 1:100 diluted exosomes or IDEM. The chamber was filled with milliQ water using a 1mL syringe avoiding bubbles until all the cell was completely filled. The laser box was then moved back inside the instrument. After checking that all the hardware info were positive, the circuit was cleaned with 1mL syringe of milliQ water. After cleaning, the area on view was verify to be the one in the middle of the circuit. For all the samples, 3 or 5 videos of 60 seconds each were performed. The sample was infused at pump flow level of 1000 until reaching the regime and then camera level and focus were adjusted until only few nanoparticles per each frame were seen green (meaning saturation of signal) and there was maximum one halo around each nanoparticle. The measurement was performed at pump flow level of 100. After that all the setting was done, the measurement started. Once the videos were filmed, a post-processing phase was done, in which a

threshold was set in order to have all the nanoparticles tracked without considering all the debris and fragments that can only interfere with the measurements. Between each sample to be measured, the circuit was cleaned with syringes of MilliQ water at flow level 1000 and at maximum camera level until no evident nanoparticles could have been seen in the screen. At the end of the measurements, the procedure of cleaning was repeated and two syringes of air were added. The machine and the computer were turned off and the circuit was gently disassembled from the laser chamber, cleaned and left on the chamber with a napkin in between.

#### **4.4.2. Scanning electron microscopy (SEM)**

##### **4.4.2.1. Physical principle**

Scanning electron microscopy (SEM) is a technique used for imaging of surfaces of solid objects. The high resolution (10nm lateral resolution, 10 nm depth resolution) make it a really fundamental way of imaging in nanomedicine. This is due by the fact that SEM exploit electrons to make images instead of light as in the optical microscope, so we can make images at high resolution of all the samples with dimensions under the wavelength of visible light. In a chamber with vacuum (to avoid any interference to the electron pathway), an electronic beam is generated and accelerated by the anode, then it's focused by a succession of electromagnetic lenses. In **Figure 4.4.2.1** [46] it's possible to see a block diagram of the components of a generic SEM. The electron gun hits a specific area of the specimen we want to study, which was previously coated with a nanometric film of metal to avoid electrostatic interference [46], and it scans line by line. The interaction between the beam and the electrons on the surface of the sample gives many signals: backscattering electrons (BSE), X-rays and secondary electrons (SE). The first and last ones will be detected for imaging, amplified, filtered and displayed real time in a computer. BSE belong to the electron beam and they are reflected elastically by the sample and they give us information about the deepest regions, whereas SE origin

from the atoms of the sample as a result of a non-elastic interaction and they give detailed information about surface shape.

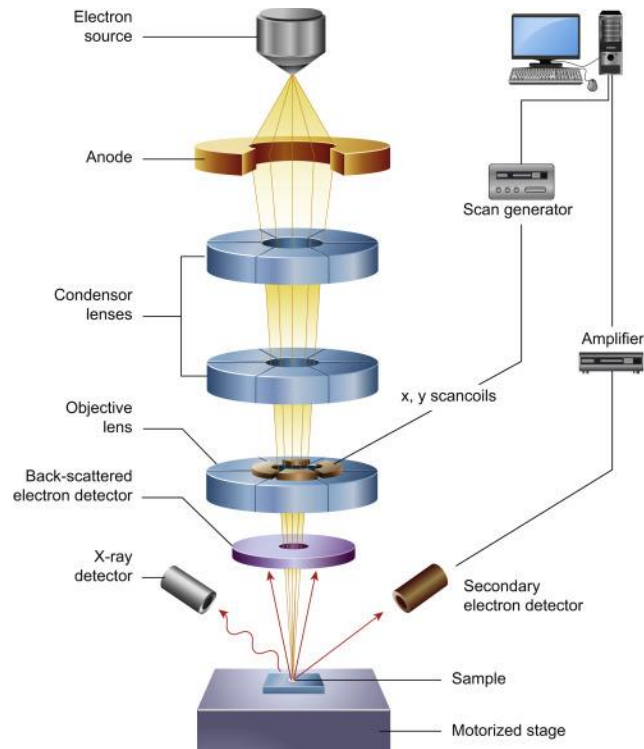


Figure 4.4.2.1: block scheme of a SEM. The main parts are the electron source, the three detectors (back-scattered detector, X-ray detector and secondary electron detector) and the amplifier of signal.

#### 4.4.2.2. Protocol

For SEM analysis, 50 $\mu$ L from each sample were placed in different 60mm\*15mm Cell Culture Petri Dishes and they were left overnight in 4C fridge with water to avoid evaporation. The next day, 2.5% glutaraldehyde was added on every sample for 10 minutes at 4C. After discarding the solution, samples undergo increasing percentage of ethanol baths (30-50-70-90-100% EtOH) for 5 minutes each at room temperature. As last bath, the samples were immersed in 50% butanol for 5 minutes. A 2cmx2cm fragment of the Petri dish was mounted with a double side carbon tape (Ted Pella Inc. USA) on an aluminum SEM (scanning electron microscope) stub (Ted Pella Inc. USA). A 5nm to 7nm thick Iridium film was coated on the sample to enhance image contrast. The SEM used in the experiment is a

system of Nava Nano SEM 230 (Thermal Fisher, USA). All SEM experiment was under condition of both a room temperature (22°C) and a high vacuum range of  $5 \times 10^{-6}$  to  $2 \times 10^{-6}$  Torr. The SEM accelerator voltage was set at 5kV to 7kV for imaging. The spot was set at 3 (nm) for imaging (the diameter of the e-beam is at 3nm). The SEM work distance was 5mm.

## 4.5. Protein content characterization: western blot

### 4.5.1. Physical principles

Western Blot (or immunoblot) is a commonly used and well-known semi-quantitative technique for protein characterization. It is based on separating proteins on a polyacrylamide gel according to their molecular weight and on detecting a protein by using specific antibodies that emit a chemiluminescent signal. Proteins are denatured and put in a gel for electrophoresis. As shown in the scheme in **Figure 4.5.1** [48], the gel is transferred to a paper that will be put in a bath with primary antibody, which binds to the specific proteins of interest. The detection will be possible only with a second bath with secondary antibody conjugated with a chemiluminescent dye.

More in detail, a known quantity in  $\mu\text{g}$  of denatured proteins are loaded in an SDS-PAGE porous gel (sodium dodecyl sulfate–polyacrylamide gel electrophoresis). The gel is inserted in an electrophoresis system, constituted by an electrolytic cell immersed in running buffer. A difference of potential between anode and cathode allows to separate proteins based on their electrical charge (proteins are negative-charged, so they are attracted to the positive pole). The higher the molecular weight, the shorter distance in the gel it runs across. A protein standard with 10 pre-stained chromophore-conjugated recombinant proteins covering a wide range of molecular weights (from 10 to 250 kDa) is also loaded to permit the deduction of molecular weight [48]. Subsequently, the gel is transferred in a PVDF membrane using the same system of electrophoresis, but with transfer buffer and a “sandwich-like” system, as specifically reported in

**Figure 4.5.1** [48]. The membrane is then cut to allow for multiple detection of proteins and immersed in blocking buffer which is solution of proteins that passively adsorb to all the remaining bindings surfaces of the plate. It is used for reducing background noise [49]. Lastly, the membrane is immersed in antibody solution overnight. The next day, the samples are conjugated with secondary antibody, damped with chemiluminescent dye and detected.

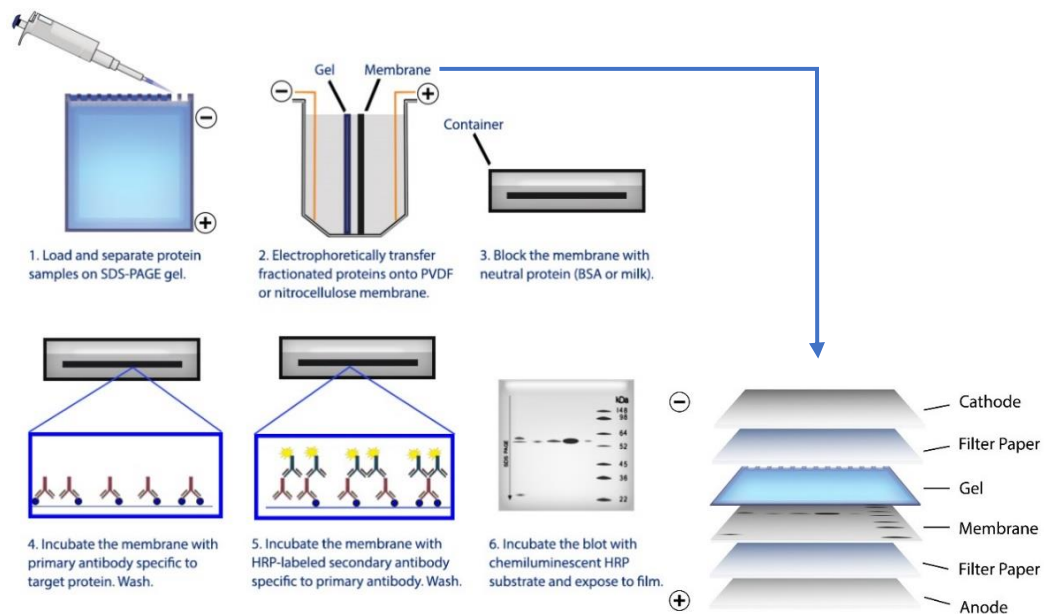


Figure 4.5.1: block scheme of the main passages of Western Blot Analysis and detail of “sandwich-like” membrane.

#### 4.5.2. Protocol

After exosomes and IDEM preparation, samples were prepared for protein extraction and quantification. The pellet of each nanoparticle was resuspended in 80 $\mu$ L of lysis buffer (made of 1 $\mu$ L of phosphatase-protease and 100 $\mu$ L M-PER). The samples were sonicated for few seconds and kept on ice in an ice bucket, which was put on shaker for 30 minutes at a sustained spin level. Every 5 minutes the samples were vortexed. Sequentially, they were centrifuged at 14800rpm for 10 minutes to remove cell organelles and debris, then the supernatant was transferred to clean vials and 4 $\mu$ L were used for Bicinchoninic Acid Assay (BCA). The protein

quantification assay was done by following the Bio-Rad DC Protein Assay protocol for determining protein concentration and Pierce™ BCA Protein Assay Kit protocol for the standard curve. The measurement was done in order to have the same amount of proteins for all the samples.

Regarding Western Blot (WB) protocol, M-PER Mammalian Protein Extraction Reagent was purchased by ThermoFisher Scientific; buffer ingredients, molecular weight ladder (4μL needed for one run), Mini trans-blot filter papers, Mini Protean Gels and Electrophoretic chamber from Bio-rad; the Amersham Protran 0.1μm Nitrocellulose Blotting Membrane from GE Healthcare Life Sciences. Primary antibodies were provided by Santa Cruz Biotechnology (ALIX and CD81), abcam (TSG-101 and CD9) and Thermo Fisher Scientific (CD63).

The primary antibody solutions were done by following the dilutions written in every datasheet with Bovine Serum Albumin-tris-buffered saline (BSA-TBST 1X). The secondary antibody solution was prepared in function of the type of primary antibody that was used (mouse, rabbit) in dilutions 1:2000 in BSA-TBST 1X. For the imaging protocol, Pierce ECL Western Blotting substrate (Peroxide solution and Luminol Enhancer solution) were provided by ThermoScientific.

Transfer buffer was made by 700mL milliQ water, 200mL methanol, 100mL TRIS-glycine 10X (purchased from X Fisher Bioreagents) and it was reusable up to three times. Running buffer was made by diluting 10 times Tris-glycine SDS buffer 10X in water. Loading buffer (LB) was prepared with a dilution 1:20 of β-mercaptoethanol and LDS (LDS buffer no reducing 4X, ThermoScientific), respectively. Blocking solution was done with 5%BSA in TBST 1X and stored at 4°C.

6μL of LB were added to all protein samples, then M-PER to fill up to 24μL (for well with 30μL of capacity). Samples were then heated at 95°C for 5minutes in agitation and quickly centrifuged for few seconds to remove bubbles.

Afterwards, the electrophoresis system was assembled with the gel and verified of no leakage. The chamber was then filled with running buffer. All

the protein samples and the ladder were loaded in the wells. 5 minutes at 120V and subsequently 45 minutes at 180V were imposed. During the running time, the gel was always kept wet in the buffer and all the system was put in an ice bucket.

After this phase, all the chamber was emptied, and the gel was removed from the electrophoresis system. The plastic container of the gel was broken gently and the gel was put in a "sandwich-like" structure made of two wet sponges, a Whatman paper, protran paper, the gel, Whatman paper and two other sponges. With a roller all the bubbles were removed from the sandwich. During all the procedure, it was made sure that all the layers were wet by transfer buffer. The sandwich was then closed and put in a transfer box (with proper direction), then it was inserted in the chamber filled with cold running buffer (ice was put inside and outside the chamber). The system was run at 200mA for 70-80 minutes.

After it, the membrane was cut using a scalpel in the proper zones for the primary antibody baths. All the passages were done in wet conditions. 3-3.5mL of blocking solution were then added to each stripe and the container with all the stripes was left under mild shaking for 1 hour at room temperature. After removing the blocking buffer, antibody solutions were added, and all the stripes were incubated overnight at 4°C under agitation. The next day, primary antibody solutions were collected, and the stripes were washed three times with 6mL TBST1X under sustained shaking at room temperature.

Afterwards, incubation with 4mL secondary antibody solution was done for 1 hour at room temperature in mild agitation. The stripes were then washed with the same method mentioned before.

Stripes were then ready for detection protocol. Right before the measurement with the machine Molecular Imager ChemiDoc XRS+ (purchased by Biorad), each stripe was wetted with 400µL of a mix of two Detection Reagents and incubated in dark for 1 minute. The detector was then put in the detector for colorimetric and chemiluminescent imaging.

## 4.6. Flow cytometry

### 4.6.1. Physical principles

Flow cytometry is a cell biology technique that uses the dispersion of a laser beam (monochromatic light) when it hits cells or other particles in order to count, classify and distinguish them in heterogeneous suspensions [50]. Solutions are placed in a sample tube inside the instrument and forced to pass rapidly flowing (more than 10,000 cells/s) into a single-file hydrodynamically focused liquid stream [51]. The beam is collimated, focused on flow chamber by multiple lenses. Every particle with a size between the wavelength range of the laser beam hits and scatters the laser in a precise region of the machine called “interrogation point”, where we can find the following detectors:

- Forward Scatter or Front Dispersion detector (FSC), placed in line with the laser, made by a lens and a photodiode for scattered light and a mirror for retention of direct light. It gives information about the volume of the particle;
- Side Scatter or Side Dispersion detectors (SSC), located laterally (usually at 90° from the laser beam), constituted by lenses that focus the lateral scattered light on a dichroic mirror, allowing only the same wavelength of the source to be reflected and so to be detected. It gives us information about the internal complexity such as granularity, shape of the nucleus, roughness of the cell [52];
- Lateral Fluorescent detector (SFL), that can distinguish different fluorophores from the non-reflected light of the side dispersed light after passing through an interferential filter. It is useful for detection of particular structures, compounds or cellular functions labeled with a fluorochrome inside and on the surface of the particle. A fluorochrome is a chemical molecule that whenever it's excited with a specific wavelength, it absorbs a photon that it's re-emitted at higher wavelength of the source, showing a fluorescent signal [53].

A photomultiplier acquires the light signal in order to process it. On screen there will be a histogram (one parameter) or a Cytogram (two parameters).

In **Figure 4.6.1** [54], a scheme of the basic functions of flow cytometer is shown. For our experiments, the machine Fortessa/LSR was used.

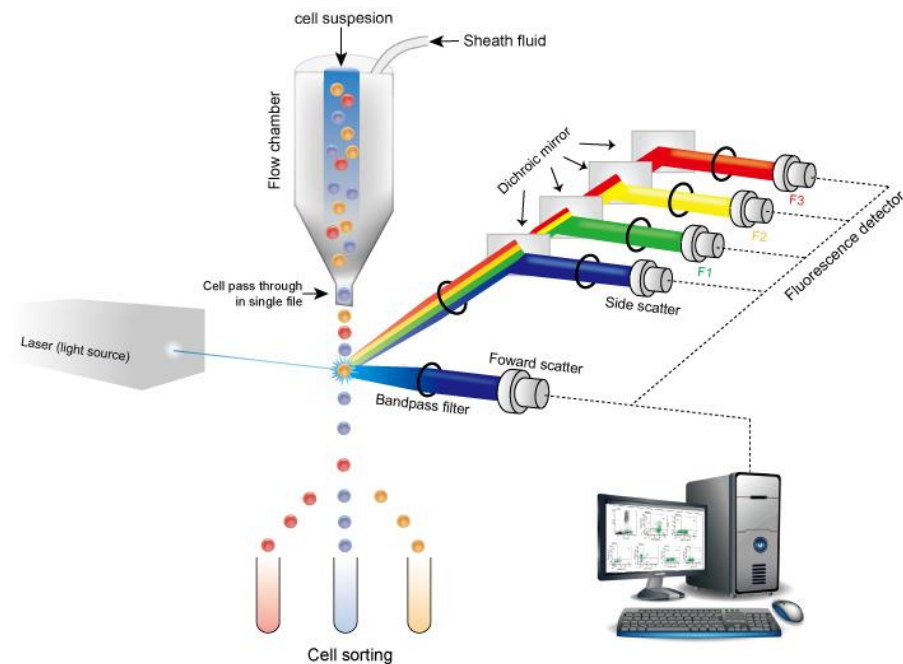


Figure 4.6.1: block scheme of a generic flow cytometer. The main parts are shown such as light source, flow chamber, FSC, SSC, SFL, dichroic mirrors and a computer for data processing

#### 4.6.2. Protocols

Since exosomes and IDEM are too small to be clearly detected and analyzed with flow cytometer, the following protocol has been used to stain them with latex Beads from Aldehyde/Sulfate Latex Beads, 4% w/v, 4 $\mu$ m, stored at 4°C fridge. The ratio exosome/beads is around 125:1. Beads were vortexed to resuspend them. In a 1.5mL Eppendorf tube, 5 $\mu$ L stock beads (corresponding to 8x10<sup>6</sup> beads) and a sample of minimum 10<sup>9</sup> exosomes (calculated from the concentration measured from NTA) were mixed. The sample was left for 15 minutes on ice in agitation and mixed every 5 minutes. Later, 0.22 $\mu$ m filtered PBS was added up to 1mL and the sample was incubated overnight in agitation at 4°C. Untreated Aldehyde/Sulfate beads were used as a negative control.

The next day, 100mM glycine solution was added to saturate unbound beads and left incubating for 30 minutes at room temperature. The obtained solution was then divided in a number of staining and unstaining. The solutions were

centrifuged for 5 minutes at 4000rpm. The supernatant was removed without disturbing the pellet. From this point, only the stained samples were processed. From the 4°C fridge, 1µL of only human or mouse fluorescently labelled antibody (FITC for CD9 and APC for CD81, chosen in order to avoid overlapping of fluorescent signal, provided by Invitrogen) was taken and added to every 100µL of diluent (2%FBS+PBS, 100µL of diluent for every type of staining to do). 100µL were added to every sample to be stained. Then, 500µL of diluent were added to all the samples, both stained and unstained and incubated for 30 minutes at room temperature in dark.

For the preparation of compensation, one drop from each of the two Versacomp antibody reagents were mixed for every needed compensation. Then, 1µL of each antibody was added and the solution was incubated for 10 minutes in dark on ice. After this time, 200µL of diluent was added. All the samples were then transferred into tubes for flow cytometry and left in dark. Analysis was performed afterwards.

Flow cytometry was also used for cellular uptake analysis of doxorubicin-loaded exosomes and IDEM into SKOV3 cells by using the following protocol.

100,000 SKOV3 cells were seeded in 12multi-well plate with 800µL of media. The next day, 1µg/mL and 3µg/mL doses of dox-loaded exosomes and dox-loaded IDEM were injected, together with the control with doxorubicin and the control without any nanoparticle. The experiment was set to have three time points, 2-4-12 hours from injection, so at each time point a well of each type of treatment and controls were prepared. At every time point, the cells of the four selected wells were detached with 500µL of triple-X100, then they were resuspended with media and centrifuged at 300xg for 5 minutes. The supernatant was removed and the cell pellet was resuspended in 200µL of PBS-1%FBS to wash them. For the analysis, the same machine mentioned above was used, exploiting the autofluorescence of doxorubicin at excitation of 480nm and emission at 590nm.

## 4.7. Test 2D drug cytotoxicity and cell viability assessment

### 4.7.1. Physical principle

Alamar Blue is a reagent that allows to quantitatively measure cell viability in a non-toxic way. In fact, its main component resazurin is involved in cellular REDOX reactions that make it change color from blue to pink, the typical color of reduced form of resazurin (resorufin). The REDOX of resazurin is detectable both with fluorescence (excitation 530nm-560nm/Emission 590nm) and absorbance (value at 570nm normalized to the one at 600nm) [54]. In **Figure 4.7.1 a** [56] we can see the spectra of resazurin in both types of detections and in **Figure 4.7.1 b** [56] the chemical reaction.

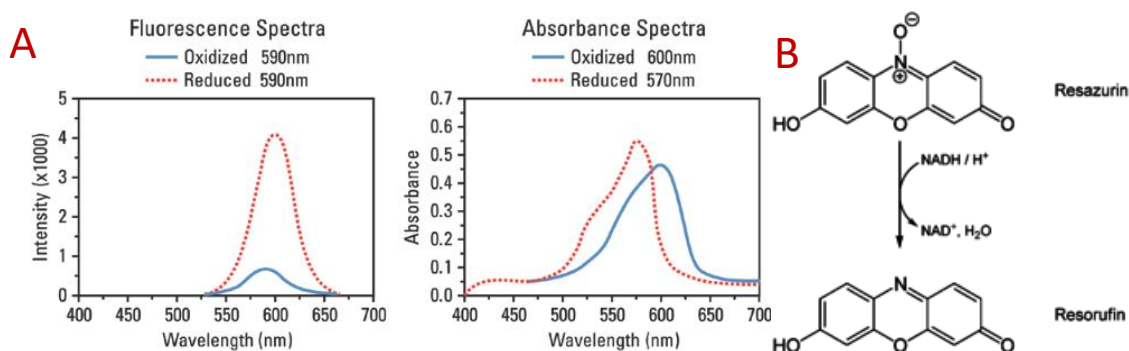


Figure 4.7.1: Resazurin characteristics. a) Fluorescent and absorbance spectra. b) Chemical reaction scheme that provoke the change of color that allow us to quantify cell viability.

### 4.7.2. Protocols

For drug cytotoxicity testing, Alamar Blue cell viability assay was performed following the protocol of AlamarBlue cell viability Reagent provided by Invitrogen. 10,000 SKOV3 were seeded per each well of a 24well multi-well plate (Nunclon Delta Surface, provided by ThermoScientific) with 500 $\mu$ L of cell media. Different doses of most common chemo drugs for *in vitro* testing were used, as shown below:

- PACLITAXEL  $\rightarrow$  0.01-0.1-1-3-10 $\mu$ g/mL [57][58][59]
- CARBOPLATIN  $\rightarrow$  10-30-100-300-1000 $\mu$ g/mL [57][60]
- DOXORUBICIN  $\rightarrow$  10-25-50-100-150 $\mu$ g/mL [61][62]

After 24 hours from cell seeding, the different doses were administered to the cells. Every 24 hours, the protocol of Alamar Blue was followed to quantify cell viability. All the doses were done in triplicate as the control (SKOV3 without any treatment) as well as all the withdrawals for Alamar Blue measurements. After 2 hours of incubation with Alamar Blue, 100 $\mu$ L from each well were withdrawn and placed in a Costar assay 96-well plate (Black with Clear flat bottom, provided by Corning). After the measurement, all the wells were washed with 550 $\mu$ L of PBS and the treatment was re-injected with fresh media following the same dilutions mentioned above. The test was pursued for 96 hours.

Regarding cell viability test, it was performed of SKOV3 cells, an ovarian cancer cell line derived from the ascites of a 64-year-old Caucasian female with an ovarian serous cystadenocarcinoma [63] in order to do a preliminary 2D study about the impact of dox-loaded exosomes and IDEM in ovarian cancer cells viability.

For testing cell viability with dox-loaded exosomes and IDEM on SKOV3 cells, Alamar Blue cell viability assay was performed following the protocol of AlamarBlue cell viability Reagent provided by Invitrogen. 6,000 SKOV3 were seeded per each well of a 96-well multiwell (Cellstar, provided by Greiner bio-one) with 200 $\mu$ L of cell media. Doses of exosomes and IDEM were taken based on EE% data. Three doses were tested for both exosomes and IDEM, that are 1-3-5 $\mu$ g/mL. The controls were:

- EXO and IDEM nanoparticles no dox-loaded: starting from the concentration of nanoparticles in dox-loaded samples that was found with nanosight analysis, the number of nanoparticles in the specific dose was found, then an equivalent number of exosomes (in suspension) were taken from non-loaded batches, equally based on NTA analysis (EXO CTRL-IDEM CTRL);
- SKOV3 cells with 10 $\mu$ g/mL of free doxorubicin (DOX);
- SKOV3 cells without any treatment (CTRL).

The procedure that was followed is then the same explained previously, whereas in **Figure 4.7.2** a block scheme of the protocol is shown.

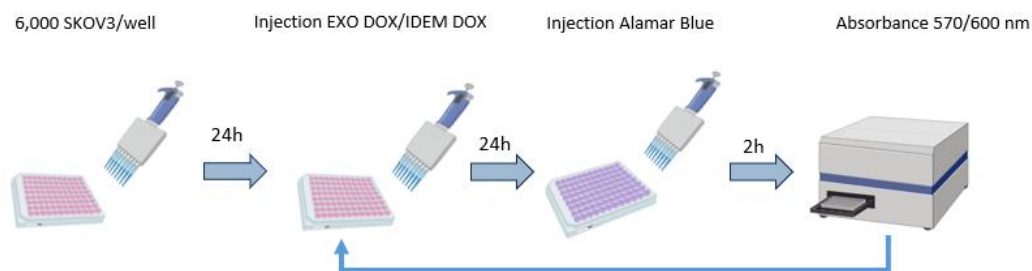


Figure 4.7.2: Block scheme of Alamar Blue protocol followed for cell viability test on SKOV3 with dox-loaded exosomes and IDEM treatment

#### 4.8. Encapsulation efficiency (EE%)

Different methods of doxorubicin-loading (DOX-loading) were compared in order to obtain a reliable and consistent encapsulation efficiency value. After evaluating 2h incubation with doxorubicin at 37°C in agitation 200 rpm, cycles of ultrasonication and 2h incubation at 37°C in agitation 200 rpm; saponin at different percentages and 5 min incubation with doxorubicin at 37°C in agitation 200 rpm, the choice fell on the last method in order to make fast and sterile nanoparticles. 5mg of doxorubicin powder were hydrated in 1mL of PBS, making a stock of 5mg/mL, whereas 100mg of saponin powder were hydrated with 10mL of PBS, making a stock of 1% m/v. The encapsulation efficiency of the nanoparticles after loading them with 400µg/mL of doxorubicin and using 0.1% v/v and 0.2% v/v of saponin respectively were compared. The concentration of 0.2% was found in literature [64]. After pipetting to mix all the components, the samples were left in agitation 200rpm at 37°C in dark for 5 minutes. Consequently, an Exosome Spin Column (MW 3000-Invitrogen-Thermo Fisher Scientific) was employed for each sample to remove unencapsulated doxorubicin. Triton-X100 (1:1000 diluted and vortexed) was added to the samples reaching 350µL in order to disrupt the remaining nanoparticles and to release the encapsulated doxorubicin in them. After shaking the samples for 10 minutes, triplicate of 100µL were used to check for Doxo concentration.

In order to prepare a Doxo calibration curve, dilutions from a stock of 5µg/mL of Doxorubicin in PBS were performed. The specific concentrations that were used are shown in **Table 4.7** (other than PBS only).

| Dilution   | Volume of PBS [ $\mu\text{L}$ ] | Volume of Doxorubicin [ $\mu\text{L}$ ] |
|------------|---------------------------------|---|
| 5          | 0                               | 350                                     |
| 2          | 210                             | 140                                     |
| 1          | 280                             | 70                                      |
| 0.5        | 315                             | 35                                      |
| 0.2        | 336                             | 14                                      |
| 0.142857   | 340                             | 10                                      |
| 0.1        | 343                             | 7                                       |
| 0.07142857 | 345                             | 5                                       |

Table 4.8: List of dilutions used for doxorubicin calibration curve.

Using the machine Synergy H4 hybrid plate reader and the software Gen5, the auto-fluorescence of Doxorubicin was detected with Excitation wavelength of 480nm and emission of 590nm, based on doxorubicin spectrum found in literature [65] and shown in **Figure 4.8** [66].

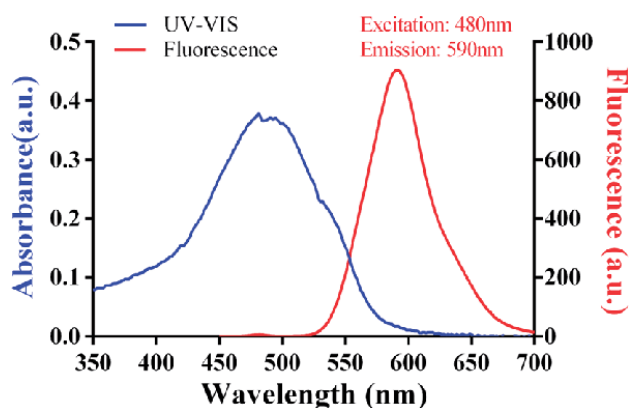


Figure 4.8: Absorbance and Fluorescence spectra of Doxorubicin

#### 4.9. Drug release (DR%)

The drug release profiles of both EXO and IDEM were studied in parallel. EXO and IDEM were dox-loaded following the 0.1% saponin protocol explained in section 4.8. Samples were then injected in the center of two different Snakeskin Dialysis Membranes (10,000 MWCO 22cmx35 feet dry diameter, prod 68100) of 11cm length that were subsequently folded in half and the extremities were clipped together

with SnakeSkin Dialysis clips. Each membrane with sample was immersed in a 50mL beaker with 20mL of PBS heated at 37°C on an Isotemp stirring hotplate (provided by ThermoFisher Scientific) with a magnetic stirring bar at 350rpm. The beaker was covered with multiple parafilm tape in order to avoid evaporation of water during the experiment. To complete the setting, both structures were covered with Aluminum foil to protect from the light. Monitoring of drug release was performed at the following time-points: 0-0.5-1-2-4-8-12-24-48-72-96 hours. At each time point, 1mL of liquid was withdrawn from each beaker for measurement and replaced with 1mL of 37°C-heated fresh PBS. Each withdrawal measurement, as well as the calibration curve, was done in triplicate by adding 300µL to each well of a Costar assay 96-well plate (Black with Clear flat bottom, provided by Corning), covered with aluminum foil. Regarding the calibration curve preparation, subsequent 1:2 dilutions starting from a stock of 5µg/mL of Doxorubicin in PBS were performed. The specific concentrations that were used are shown in **Table 4.9** (other than PBS only).

|            |                 |
|------------|-----------------|
| Dilution A | 2.5µg/mL        |
| Dilution B | 1.25µg/mL       |
| Dilution C | 0.625µg/mL      |
| Dilution D | 0.3125µg/mL     |
| Dilution E | 0.15625µg/mL    |
| Dilution F | 0.078125µg/mL   |
| Dilution G | 0.0390625µg/mL  |
| Dilution H | 0.01953125µg/mL |

Table 4.9: List of dilutions used for doxorubicin calibration curve.

At each time point, the fluorescence of the sample was detected as written the section 4.8. After 96 hours, remaining sample in the snakeskin was removed, the volume was recorded, then Triton-X100 (1:1000 diluted) was added to reach 1mL in order to disrupt the remaining nanoparticles and so to release the encapsulated doxorubicin in them. After shaking the samples and left them rest for 10 minutes, triplicate was done as for the previous time points and for detection, the same procedure written in section 4.8 was performed.

To find the cumulative drug release, the following equation was used:

$$(b) \quad DR\% = \sum_{n=1}^{n=t} \frac{(C_n \cdot V - C_{n-1} \cdot v)}{m_0} \cdot 100$$

With  $t$  number of time points which goes from 1 to 10,  $C_n$  concentration of doxorubicin at time  $t$ ,  $V$  the total volume of liquid (in our case 20mL),  $C_{n-1}$  concentration of doxorubicin at time  $t-1$ ,  $v$  non-withdrawn volume (in our case 19mL),  $m_0$  the mass of doxorubicin in the nanoparticles. In **Figure 4.8**, the workflow of the protocol is shown.

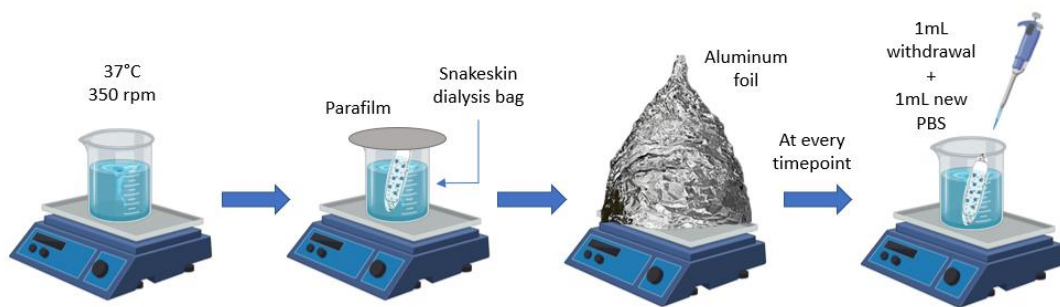


Figure 4.9: Schematic workflow of the drug release profile protocol analysis

## 4.10. E-sight

For cell viability, the opportunity to collaborate with the enterprise Agilent was possible by using the xCELLigence RTCA eSight machine (eSight). The eSight machine provides label-free, real-time biosensor impedance-based measurements and kinetic imaging of a live cell population simultaneously, it monitors cell health and adhesion, morphology, proliferation, cytolysis, imaging supports three fluorescent channels, 5-well plate formats and a user-friendly software is provided for monitoring and post-processing of data [67]. The machine could stay inside a wide range of incubator models [68].

### 4.10.1. Physical principle

A specialized electronic 96-well microplate is used for eSight cell viability monitoring. Every well is composed by a gold biosensor embedded with the glass bottom of the well that continuously and noninvasively monitors cellular

impedance of the cells in it, making an array of biosensor (**Figure 4.10.1** point 1, above). An electric current in the order of micro-Ampere ( $\mu\text{A}$ ) passes through the gold wire, but since cells make a resistance to the current flow, it's possible to correlate the change of impedance to the cell number, cell size, cell substrate attachment strength and cell-cell interaction strength. The user can set a temporal resolution (how frequent the impedance value is measured) in which an adimensional value called "cell index" is measured. Apoptosis/cell death bring a drop in impedance signal, while an increase of number of alive cells will increase it. As shown in the point 3 of **Figure 4.10.1**, the live cell imaging is possible thanks to fluorescent dyes (red, blue, green) [69].

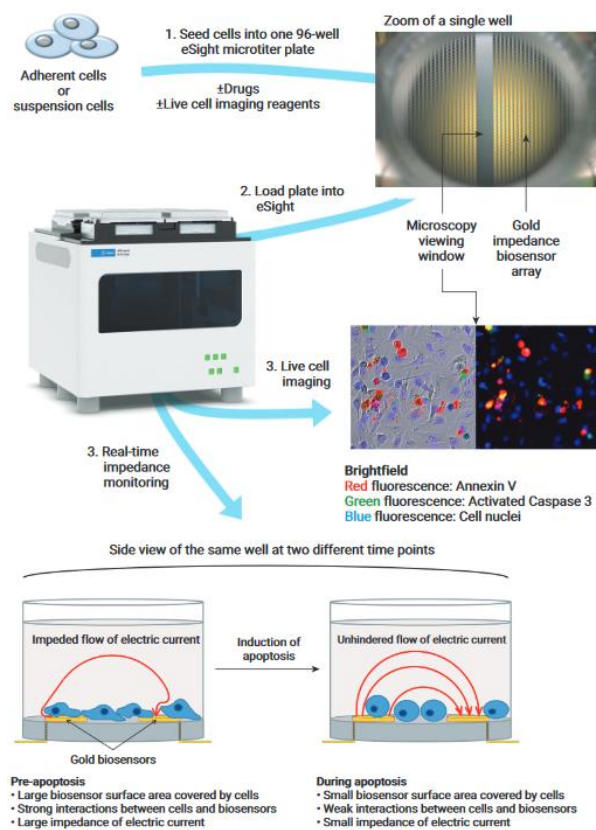


Figure 4.9.2.1: Agilent eSight workflow and features. Real-time impedance monitoring (Number 3) was used for cell viability monitoring in this work.

#### 4.10.2. Protocol

6,000 SKOV3 cells were seeded in a specialized electronic 96-well microplate with 200 $\mu\text{L}$  of media and then put in the eSight machine in incubator. After 24 hours,

the treatment was administered to the cells (dox-loaded exosomes and IDEM). Controls such as non-dox-loaded exosomes, non-dox-loaded IDEM, 10 $\mu$ g/mL free doxorubicin and no treatment, were injected, too. The multiwell was then replaced in the eSight machine in incubator for 96 hours monitoring. In **Figure 4.10.2** a block scheme of the procedure is shown.

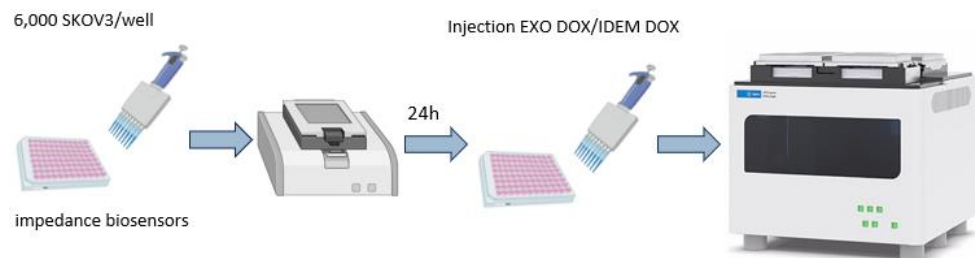


Figure 4.10.2: Block scheme of eSight protocol followed for cell viability test on SKOV3 with dox-loaded exosomes and IDEM treatment

## 4.11. Confocal microscopy

### 4.11.1. Physical principle

A confocal microscope is an optical or fluorescent microscope with improved spatial resolution of the specimen thanks to the deletion of artifacts as halos and passive phenomenon made by diffused light from the out-focus plans of the sample [70]. This is possible thanks to a pinhole between specimen and detector that selects the information from a single focal plane, producing a highly precise optical slice of the sample. By repeating the scanning at different heights, it's possible to obtain a 3D imaging [71]. There are many ways to obtain this, but the most common one uses a laser as a source of light, so it's called Laser Scanning Confocal Microscope (LSCM). It's composed by one or more laser sources of light tunable at different wavelengths, which scans point-by-point the specimen (epi-illumination); an optical pathway with pinholes, dichroic mirrors for focusing the laser beam on the sample; objectives and eyepieces; detector, photomultiplier and a computer for post-processing [72]. The oscillating mirrors scan a point of light across the specimen. The emitted fluorescence by the sample passes through a system of dichroic mirrors that reject reflected excitation wavelength. Finally, the fluorescent signal passes through the pinhole for detection. The

image is built by recording the brightness of each point. In **Figure 4.11.1** [73] a schematic view of the main parts of the confocal microscope is shown.

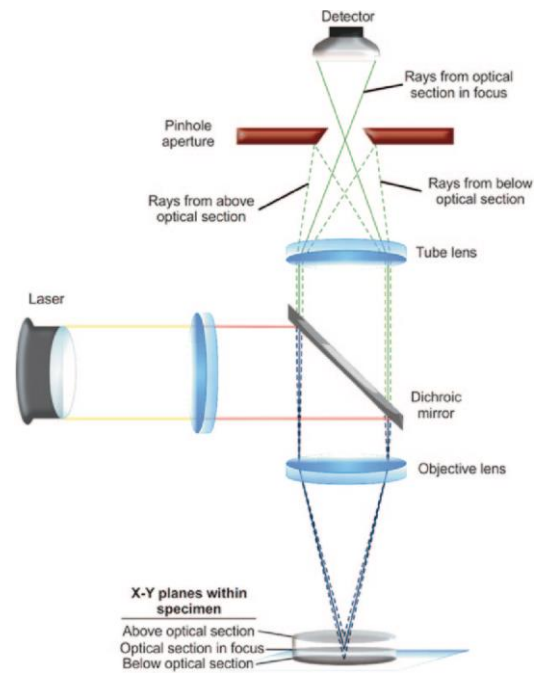


*Figure 4.11.1: Schematic view of the main parts of the confocal microscope. The heart of the system is laser and dichroic mirror, which are responsible of high laser precision, high resolution and high depth of field*

#### 4.11.2. Protocol

10,000 SKOV3 cells were seeded in 12 wells of Chamber glass slide (8 chambers mounted on glass slide with cover) in 200 $\mu$ L of media. The next day, 1 $\mu$ g/mL and 3 $\mu$ g/mL doses of dox-loaded exosomes and dox-loaded IDEM were injected, together with the doxorubicin positive control and the control without any nanoparticle. The experiment was set to have three time points, 2-4-12 hours from injection, respectively. At every time point, the cells of the four selected wells were washed twice with prewarmed PBS at pH 7.4, then they were fixed in 4% paraformaldehyde solution in PBS for 10 minutes at room temperature, avoiding any methanol containing fixative that can disrupt actin during the fixation process. Cells were then washed two or more times with PBS, permeabilized with 0.1% Triton X-100 in PBS for 3-5 minutes and re-washed two or more times with PBS. Regarding the staining with Phalloidin Alexa-Fluor 488,

a dilution of 5 $\mu$ L methanolic stock solution into 200 $\mu$ L PBS for each well to be stained was prepared. To reduce nonspecific background staining, 1% BSA was added to the staining solution. The latter was placed on the coverslip for 20 minutes at room temperature in a covered container in order to avoid evaporation. Subsequently, the sample was washed with PBS two or more times. The specimens were ready for detection. The machine used to take pictures is a "Fluoview TM3000" provided by Olympus.

## 4.12. 3D cultures and IDEM cytotoxicity

### 4.12.1. Physical principle

The 3D cancer model aims to be biologically closer to *in vivo* tumors compared to 2D *in vitro* cell culture. In fact, in 3D model tumor cells are exposed to suboptimum growth conditions such as hypoxia, low nutrient level and the interactions between cells highly influence the surrounding environment and the other cells [74]. Also, the morphology of the tumor is not the same between 2D and *in vivo* conditions, which implies that cells behavior is far from reality, for example they replicate the human solid tumor, which resist to therapeutics [75]. All these conditions are impossible to replicate in monolayer culture, which leads to an unreliability to the *in vivo* conditions. That's why 3D model is a fundamental step do to as a bridge between 2D *in vitro* and *in vivo* models [76].

The technique that was employed for creating spheroids is scaffold-free and formed without specific equipment and tools [75].

Regarding cell viability assay, CellTiter-Glo 3D cell viability Assay was used. it determines the number of viable cells in 3D cell culture by quantifying the ATP, a sure marker of metabolic activity of an alive cell. After cell lysis, the luciferase acts with luciferin and ATP and the emitted signal is linearly proportional to the amount of ATP in 2D case, curvilinear in 3D culture (**Figure 4.12.1**). This different correlation is due to the fact that spheroids usually have necrotic core and the cells in them proliferate less because of lack of cell adhesion to substrate, but by correlating the amount of RNA to the one of DNA (linear correlation), it's possible

to quantify the number of viable cells. CellTiter-Glo 3D is ready-to-use reagent, fast, highly sensitive, for every type of plate/multiwell format and it can penetrate into microtissues [77].

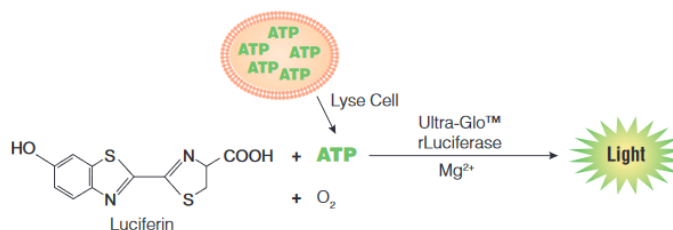


*Figure 4.12.1: chemical reaction that involves luciferin, ATP and luciferase with a resulted light signal proportional to the amount of ATP in the sample, so directly related to the quantity of viable cells.*

#### 4.12.2. Protocol

As mentioned above, spheroids were obtained using Black walled Ultra Low Attachment (ULA) plates (Corning, #4515). 5,000 SKOV3 cells were seeded in each well with 200 $\mu$ L of media. After briefly shaking, cells were incubated to permit the formation and stabilization of the spheroids. Half of the media in each well was exchanged with fresh media on alternate days. After 24 hours since cell seeding, the treatments were added as shown in the block scheme in **Figure 4.12.2**.

From 3D cell viability assessment, the CellTiter-Glo 3D Reagent assay was performed at each time point following the protocol from Promega [77]. Briefly, the reagent was heated at 22°C prior the use for 30 minutes and mixed gently to obtain a homogeneous solution, then the test compound was added to experimental wells and put in incubation. The plate was then equilibrated to room temperature for 30 minutes, the CellTiter-Glo was added in the same amount of medium present in each well (100  $\mu$ L) and the plate was vigorously shaken to induce cell lysis. The plate was then incubated for additional 25 minutes at room temperature to stabilize the luminescent signal.

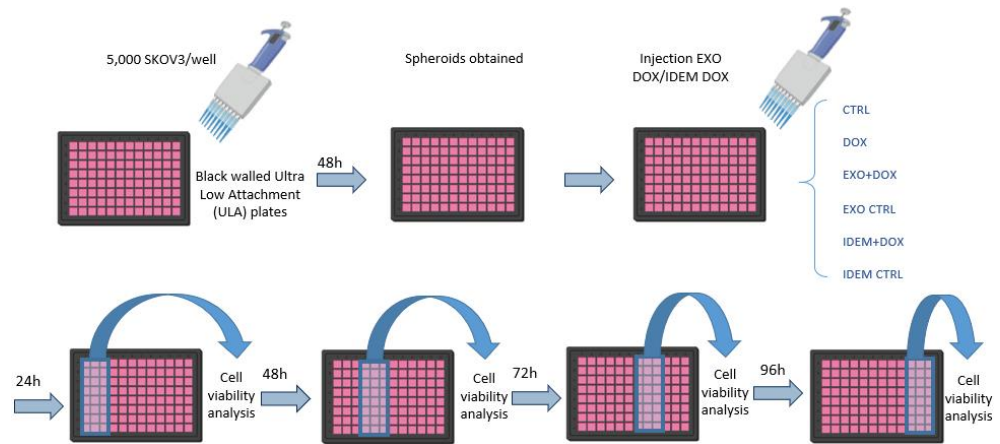


Figure 4.12.2: Block scheme of the procedure followed for spheroid cell viability assay.

### 4.13. Statistical analysis

A two-tailed Student's t-test was performed. Data with  $p < 0.01$  were considered consistent. All the graphs show median and standard deviation, whereas data with  $p < 0.001$  were considered highly consistent.

## 5. Results and discussion

### 5.1. Dimensional characterization and concentration assessment

Both exosomes and IDEM were produced as reported in sections 4.2 and 4.3. An initial characterization of size and concentration for both the formulations was performed following the protocol described in section 4.4.1.2. A scanning electron microscope (SEM) analysis was also used to visualize the particles and to confirm their size, shape and distribution. Samples were prepared as described in the protocol in 2.4.2.2.

#### 5.1.1. Nanoparticle Tracking Analysis

Data obtained from NTA provided information regarding the number of particles, the dimensional distribution and diameter of both, exosomes (EXO) and IDEM. **Figure 5.1.1 a** show their profile distribution in function of the diameter of both the particles from eleven different batches. Both nanoparticles show Gaussian profiles, with a larger diameter distribution and a higher mode for IDEM. This result is corroborated in **Figure 5.1.1 b**, where EXO and IDEM samples have an average diameter of  $112.44 \pm 14.59 \text{ nm}$  and  $177.08 \pm 19.64 \text{ nm}$ , respectively. This difference was confirmed to be statistically significant ( $p < 0.001$ ) by a T-Test analysis. In spite of the difference in diameter, IDEM still fall within the size-window that is expected from EXO and can hence be considered as exosome mimetics.

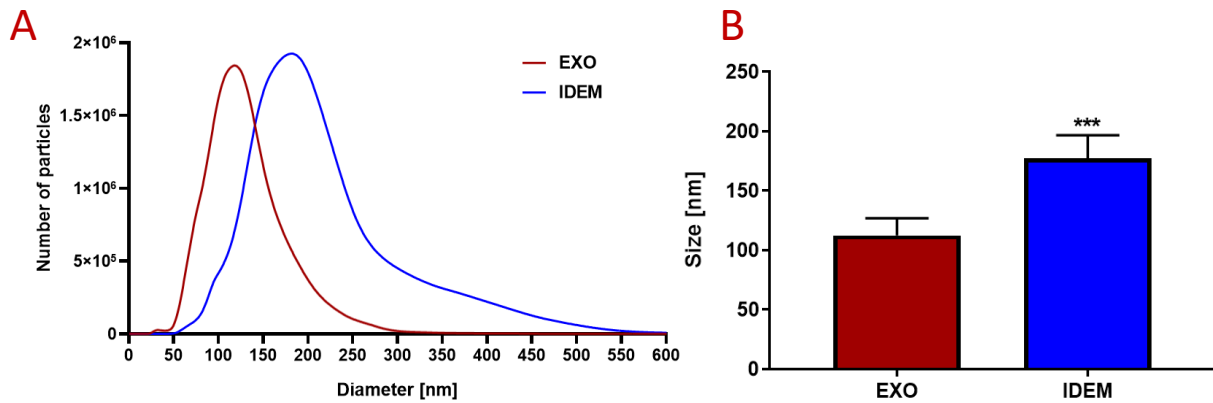


Figure 5.1.1: Size distribution analysis. A) Profile distribution of particles in function of the diameter for exosomes (in red) and IDEM (in blue) obtained by Nanosight analysis. A gaussian distribution of the particle diameter larger in IDEM samples is observed, B) Average size of exosomes and IDEM from 11 samples ( $p < 0.001$ )

**Figure 5.1.1.1** represents the concentration of particles per mL of obtained solutions in 11 bathes of both nanoparticles. Data show that  $9.42 \times 10^9 \pm 2.31 \times 10^9$  and  $2.34 \times 10^{10} \pm 7.91 \times 10^9$  particles/mL are obtained for exosomes and IDEM, respectively, which means that IDEM are 2.48 times more concentrated than exosomes, although they have been obtained from the same number of cells. This data taken all together reveal that IDEM have a size distribution that is similar to the exosome-one, which means that they are biomimetics in this characteristic, but they are also bigger, which allows to increase the possible encapsulation efficiency of drugs, chemical compounds, biological fragments etc. Also, the higher concentration of IDEM make it possible to increase the production efficiency for future scalability of production and decrease the doses to have the same number of nanoparticles.

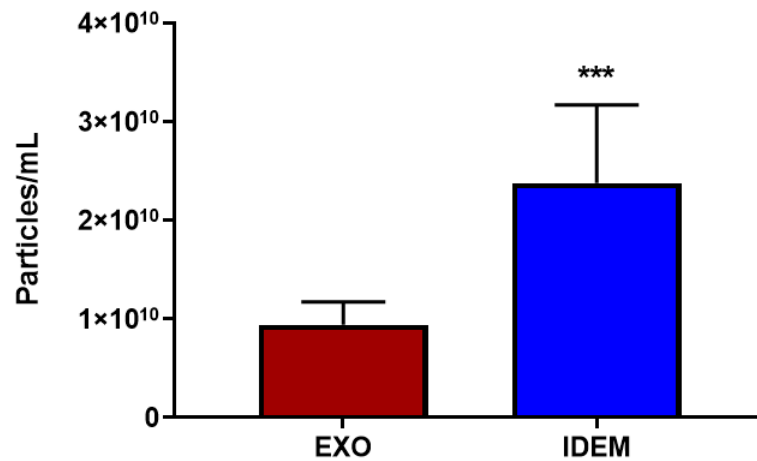


Figure 5.1.1.1: Concentration expressed in particles/mL of exosomes and IDEM according to data obtained from 11 samples by Nanosight analysis. Statistically significant differences ( $p < 0.001$ ) are observed between the two nanoparticle types, in particular IDEM are 2.48 times more concentrated than exosomes.

### 5.1.2. Scanning Electron Microscopy (SEM)

SEM analysis was fundamental to see the samples of EXO and IDEM that were synthesized. Samples were prepared following the protocol mentioned above and analysis images of significant regions are shown in **Figure 5.1.2 a** for EXO and **5.1.2 b** for IDEM. All the samples were studied at different magnifications as reported in the images. For both samples, nanoparticles with a diameter between 30nm and 175nm were found and measured. From SEM photos we can see that both nanoparticles are rounded-shaped, and the dimension distribution goes between 30nm and 180nm, but still in the range of Gaussian distribution obtained from Nanosight and in the range of exosomes dimensions.

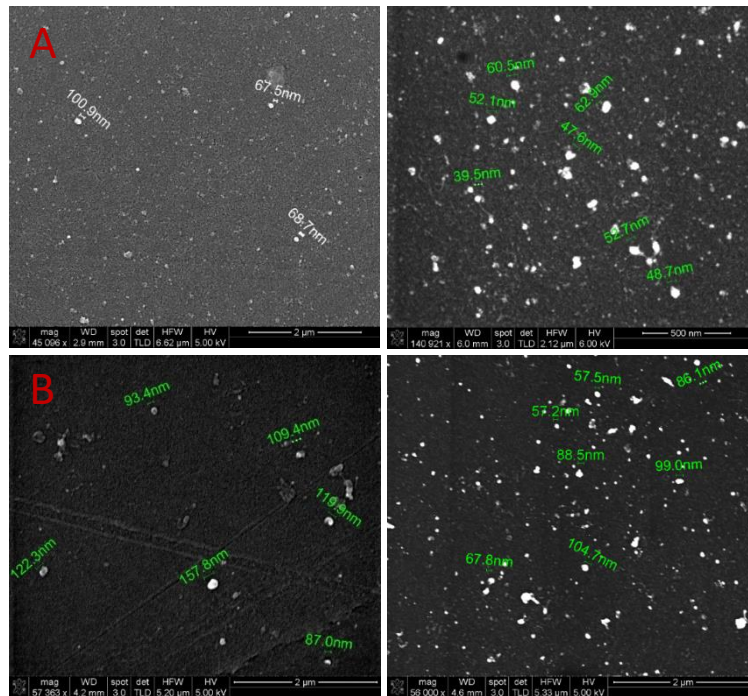


Figure 5.1.2: SEM images of A) EXO and B) IDEM at increasing magnification from left to right. Some nanoparticles measures are shown to underline the range of dimensions of nanoparticles and the gaussian distribution.

## 5.2. Protein content characterization

To verify the protein expression of IDEM and to compare it with the one of exosomes, Western blot and flow cytometry were performed. In particular, the analysis was focused on the detection of the tetraspanins CD63, CD09, and CD81, Apoptosis-Linked Gene 2-Interacting Protein X (ALIX) and Tumor Susceptibility gene (TSG101), which are typical marker of exosomes.

Molecular weights of the proteins are reported in **Table 5.2**:

|        |          |
|--------|----------|
| ALIX   | 95kDa    |
| CD63   | 30-60kDa |
| TSG101 | 44kDa    |
| CD09   | 22-27kDa |
| CD81   | 25kDa    |

Table 5.2: Molecular weight of the proteins detected.

CD63 and ALIX detection required specific optimization. Proteins were extracted and processed as specified in the protocols at section 4.5.2 and 4.6.2 respectively for western blot and Flow cytometry.

### 5.2.1. Western blot

**Figure 5.2.1** shows the results obtained from the western blot analysis. Lanes for exosomes and IDEM are shown for ALIX, CD63, TSG101 and CD09. In all the molecular range weights areas a clear expression of the proteins for IDEM is visible, meaning that IDEM express typical markers of exosomes and they could be considered a biomimetic characteristic.

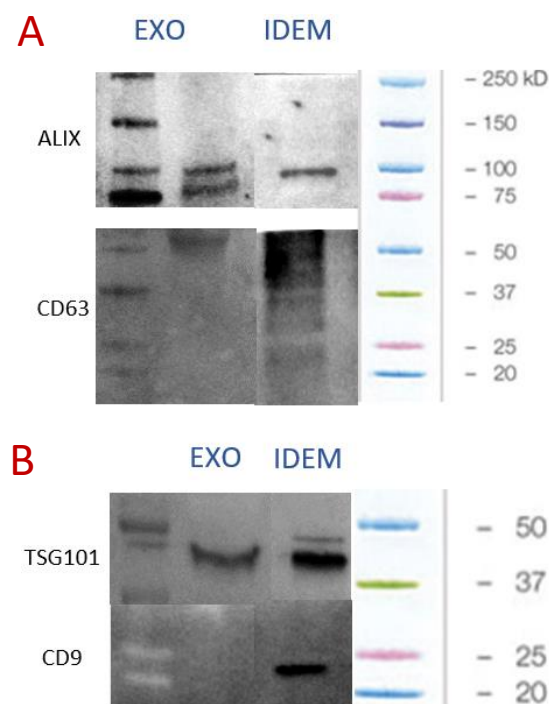


Figure 5.2.1: Western blot lanes for A) ALIX and CD63, B) TSG101 and CD09 for exosome and IDEM respectively. Signal is clear and in the range of molecular weight mentioned above in table 5.2

The signal of exosome sample is not present for ALIX and CD63. The optimization of the protocol was performed in terms of quantity of proteins and dilution of the primary antibody was performed. Results are shown in paragraph 5.2.2.

### 5.2.2. Optimization of western blot for exosomes characterization

Western blot optimization was performed with different protein concentrations (10-20-30-40 $\mu$ g) and serial dilutions of the primary antibody used (1:200 and 1:500 for ALIX, 1:250 and 1:500 for CD63). As shown in **Figure 5.2.2 a**, no signal for ALIX was detected for all the samples with 10  $\mu$ g and 20  $\mu$ g of loaded proteins regardless of the dilution. However, a light signal was observed at 30  $\mu$ g and 40  $\mu$ g for 1:500 dilution. The best signal was found to be for dilution 1:200 30  $\mu$ g and 40 $\mu$ g. As shown in **Figure 5.2.2 b** no signal is observed for 10 $\mu$ g regardless of the dilution. A slight signal for 10 $\mu$ g and 20 $\mu$ g at 1:250 dilutions, a good signal for all the other samples. For next western blot, the samples ALIX 1:200 30 $\mu$ g and CD63 1:500 30 $\mu$ g will be used.

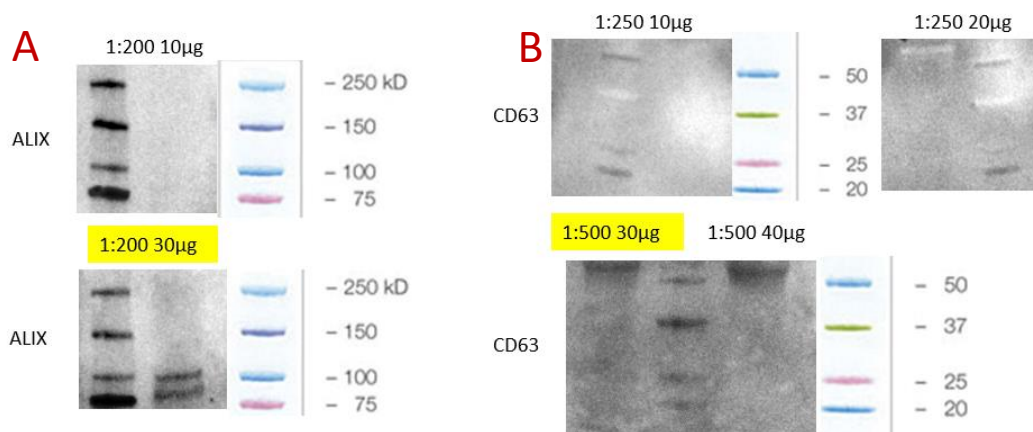


Figure 5.2.2: Optimization of Western blot for A) ALIX and B) CD63. Best signals are in the samples ALIX 1:200 30 $\mu$ g and CD63 1:500 30 $\mu$ g, which will be used for future experiments.

### 5.2.3. Flow cytometry

Regarding CD81, the results show of flow cytometry protocol for exosomes (**Figure 5.2.3 a**) and IDEM (**Figure 5.2.3 b**) below. Both samples are positive for CD81, in particular a 37% of positivity is shown in IDEM. We can deduce that IDEM express CD81 as exosomes, increasing their biomimicry.

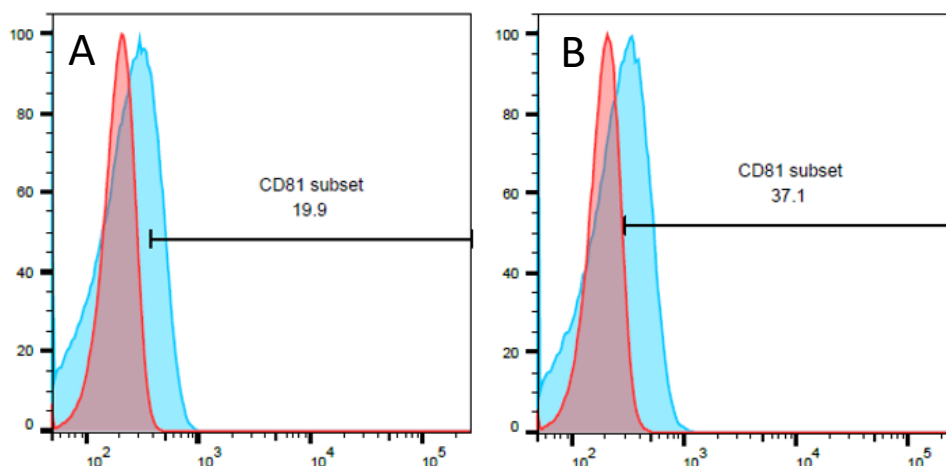


Figure 5.2.3: Results of flow cytometry for detection of CD81 for A) exosomes and B) IDEM. 19.9% of the exosomes and 37.1% of IDEM are positive for CD81

### 5.3. Test drug cytotoxicity

Three of the most common chemotherapeutic drugs (Paclitaxel, Carboplatin and Doxorubicin) were compared for their cytotoxicity potential against SKOV3 cells. Different doses (mentioned in chapter 4.7.2) were tested in order to find the best one to be used in the following experiments. In **Figure 5.3** the percentage of cell viability is reported normalized to control. Anyway, paclitaxel and doxorubicin induce cell mortality even at the lowest dosage unlike carboplatin. In particular, cell viability following the treatment with the lowest dose of paclitaxel (0.01 $\mu$ g/mL) is 60%, whereas for doxorubicin is 20%. These data led us to choose doxorubicin at the dosage of 10 $\mu$ g/mL as the positive control for the following experiments.

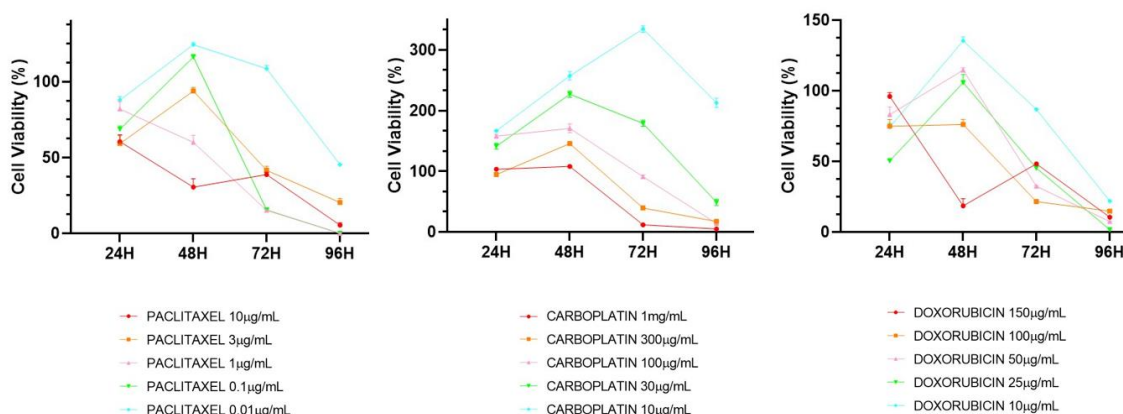
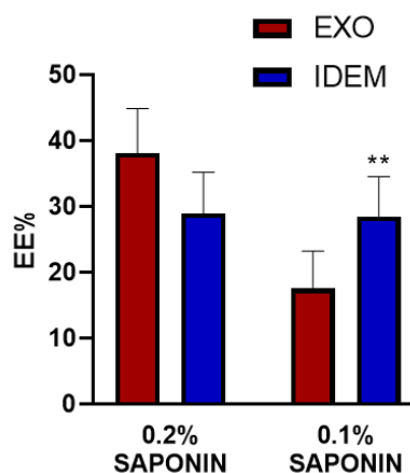


Figure 5.3: Cell viability of SKOV3 cells for three different chemotherapeutics at 5 different doses each, mentioned at section 4.7.2 and in the above legends. From left to right, data for Paclitaxel, Carboplatin and

*Doxorubicin are shown. Data were normalized to control (SKOV3 cells without any treatment). Paclitaxel and doxorubicin induce cell mortality even at the lowest dose unlike carboplatin. In particular, 10 $\mu$ g/mL doxorubicin induces 80% of cell mortality.*

## 5.4. Encapsulation efficiency (EE%)

In order to have a remarkable encapsulation efficiency, EXO and IDEM were doxorubicin-loaded (dox-loaded) and then analyzed as in the protocols described in paragraph 2.7. Two concentration of saponin were compared (0.2% and 0.1%). In **Figure 5.4** the percentage of encapsulation efficiency (EE%) is shown normalized to the initial doxorubicin concentration (400 $\mu$ g/mL). Even though the encapsulation efficiency is higher in exosome treated with 0.2% saponin, the cells that received the treatment with this percentage died after few hours. No differences were observed between 0.2 and 0.1% of saponin in IDEM. For all these reasons, the 0.1% saponin method was the chosen to proceed with the doxorubicin loading into IDEM and EXO.



*Figure 5.4: percentage of encapsulation efficiency (EE%) starting from a concentration of 400 $\mu$ g/mL of doxorubicin in each sample. At 0.1% saponin, IDEM show higher EE% than exosomes ( $p < 0.01$ ).*

## 5.5. Drug release (DR%)

The drug release (DR%, quantity of drug in  $\mu$ g/mL released, normalized to the amount of encapsulated drug in  $\mu$ g/mL, calculated with encapsulation efficiency experiment) was performed in three technical replicates. Data collected in this experiment shows the average value of DR% and the standard deviation for each timepoint (expressed in hours, over a period of 96 hours, **Figure 5.5**). Both nanoparticles show a

pronounced burst release that reaches the plateau after 12 hours. Regarding the percentage of doxorubicin released, IDEM show to release the 55% of drug after 12 hours, whereas EXO the 75%. As a consequence, IDEM have a lower burst release compared to EXO. Also, the standard deviation of EXO is larger compared to IDEM, which means that the IDEM drug release is more controllable than the one of EXO.

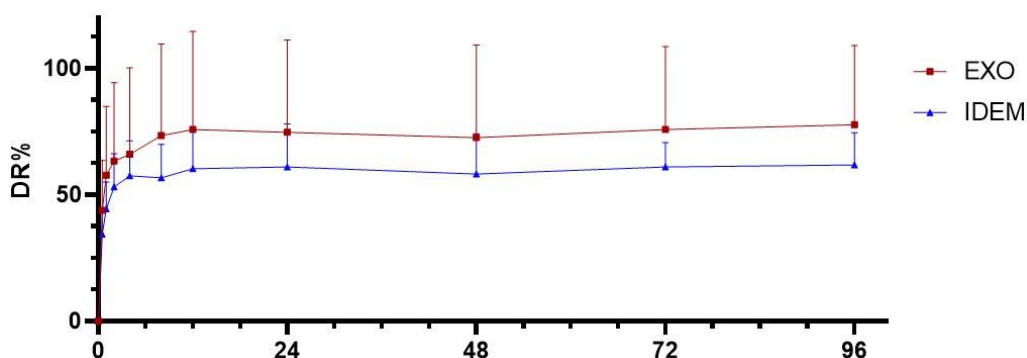


Figure 5.5: Drug release (DR%) profile of EXO and IDEM over 96 hours.

## 5.6. 2D cultures and IDEM cytotoxicity

### 5.6.1. Alamar blue

Cell viability analysis was tested on SKOV3 cells at 1-3-5 $\mu$ g/mL of Doxorubicin (DOX). In **Figure 5.6.1**, data of dox-loaded exosomes and IDEM at a)1 $\mu$ g/mL b)3 $\mu$ g/mL and c)5 $\mu$ g/mL are plotted together with the positive control (free doxorubicin, 10 $\mu$ g/mL) and non-loaded nanoparticles (EXO and IDEM). All the data are normalized to the control represented by untreated cells. From these graphs, we can deduce that at all doses, both dox-loaded exosomes and IDEM are more cytotoxic than free doxorubicin. Also, controls (EXO and IDEM without dox-loading in the same quantity of the dox-loaded doses) are less cytotoxic than the loaded nanoparticles. EXO seem to be more cytotoxic than IDEM comparing the same doses (3% and 18% of viability for EXO and IDEM, respectively in 1 $\mu$ g/mL dose, 3% and 10% for EXO and IDEM in 3 $\mu$ g/mL dose).

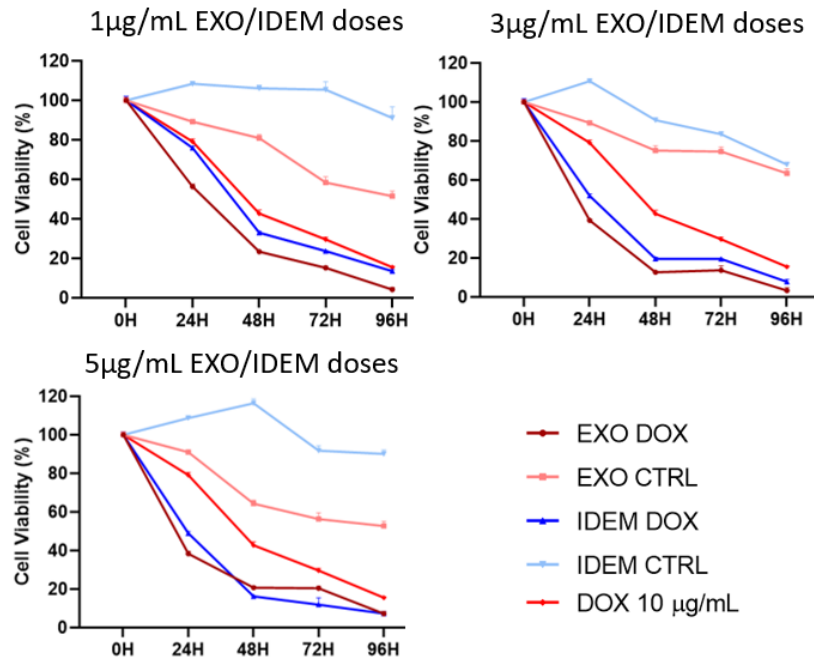


Figure 5.6.1: Data of dox-loaded exosomes and IDEM at a)1µg/mL b)3µg/mL and c)5µg/mL. At all doses, dox-loaded EXO and IDEM are more cytotoxic than the control of doxorubicin. The non-loaded EXO and IDEM show no toxicity over 96 hours. All the data are normalized to negative control (SKOV3 cells).

In **Figure 5.6.1.1** Alamar blue data normalized to the untreated controls are shown for all the three doses of dox-loaded exosomes and IDEM. At all doses, IDEM and EXO show a cytotoxic behavior after 24 hours. In particular, after 48 hours cell viability is under 40% and is further reduced to 20% at 96 hours.

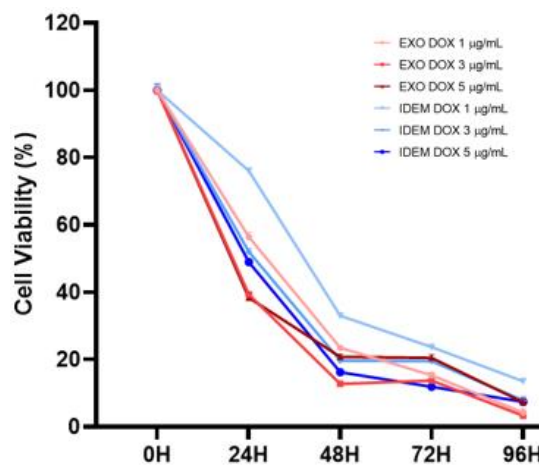


Figure 5.6.1.1: Comparison of all the doses of dox-loaded EXO and IDEM. A higher cytotoxicity is demonstrated for both nanoparticles at all doses compared to free doxorubicin. All the data are normalized to negative control (SKOV3 alone)

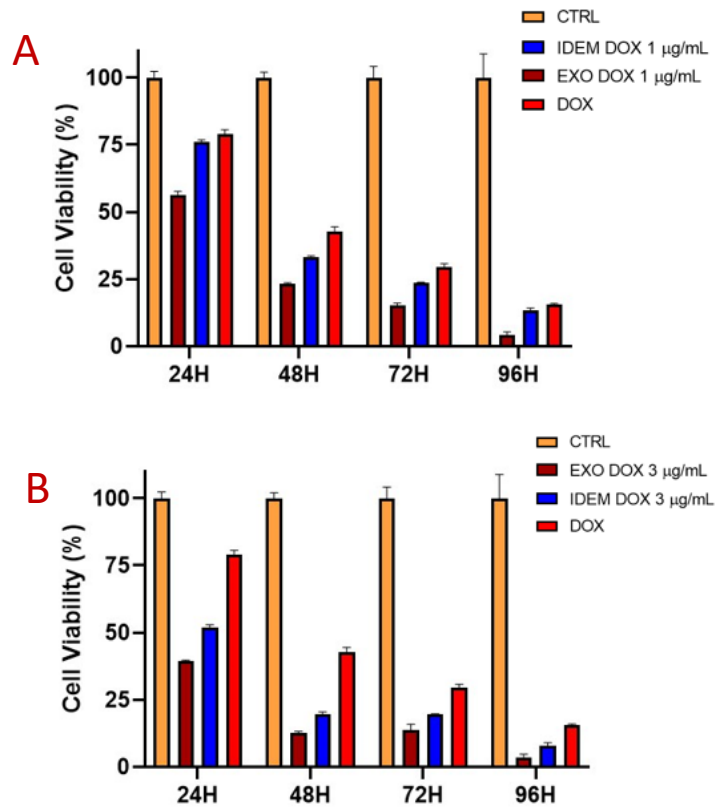


Figure 5.6.1.2: cell viability (%) of a) 1µg/mL dose and b) 3µg/mL for both exosomes and IDEM at different time points compared with free doxorubicin (DOX) and SKOV3 cells without treatment (CTRL). At all doses, both dox-loaded exosomes and IDEM are more cytotoxic than free doxorubicin. All the data are normalized to negative control (SKOV3 alone)

Lastly, a focus on the two lowest doses was done to understand their particular behavior compared to free doxorubicin (DOX). In **Figure 5.6.1.2** we can see the a) 1µg/mL dose and b) 3µg/mL for both exosomes and IDEM. We can deduce that at all doses, both dox-loaded exosomes and IDEM are more cytotoxic than free doxorubicin.

### 5.6.2. E-Sight

XCelligence eSight is an innovative machine that can make easier and more precise measurements of cell viability compared to manual and more operator-dependent cell viability procedures. For this experiment, two out of the three doses (specifically 1µg/mL and 3µg/mL) are shown. The obtained results are showed in **Figure 5.6.2** for EXO (**A**) and IDEM (**B**). Data provide information regarding the Cell Index in function of the time (expressed in hours), so the cell viability during monitoring. Data demonstrate that both dox-loaded exosomes

and IDEM have a cytotoxic behavior compared to non-loaded controls even at the lowest doses (as indicated by the cell index under 2 after 72 hours). In particular dose 3 $\mu\text{g}/\text{mL}$  is more cytotoxic than the 1 $\mu\text{g}/\text{mL}$ .

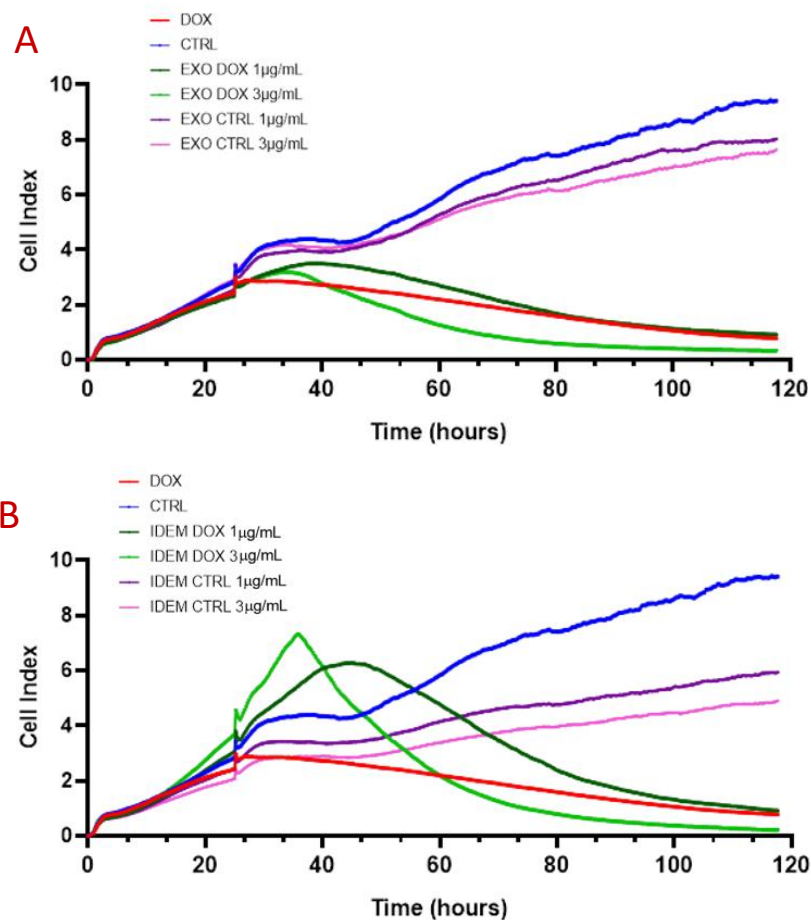


Figure 5.6.2: eSight graphs that show cell index in function of the time in hours for SKOV3 cell treated with dox-loaded exosomes and IDEM, their corresponding controls (empty exosomes and IDEM), with 10 $\mu\text{g}/\text{mL}$  doxorubicin (DOX) and untreated cells (CTRL). A) SKOV3 treated with exosomes B) SKOV3 treated with IDEM. Both dox-loaded exosomes and IDEM have a cytotoxic behavior compared to their empty counterparts.

## 5.7. Cellular uptake

### 5.7.1. Confocal Microscopy

Confocal microscopy allows to investigate cellular uptake thanks to its high resolution and low noise images and to the possibility to use fluorescent dyes to mark cell nucleus, actin cytoskeleton and doxorubicin (auto-fluorescent). Imaging was performed for 2 doses (1 $\mu\text{g}/\text{mL}$  and 3 $\mu\text{g}/\text{mL}$ ) for the both type of

nanoparticles and was compared to the positive (10 $\mu$ g/mL free Doxorubicin, DOX) and negative CTRL (untreated cells).

In **Figure 5.7.1**, images at x40 magnification are shown at the three timepoints considered the study, 2h, 4h, and 12h).

After 2 hours, doxorubicin is in the nucleus, both in cells treated with dox-loaded EXO and IDEM. In particular, at 3 $\mu$ g/mL the signal persists until 12h, so the nanoparticles are uptaken from the cells till the nucleus. We can conclude that IDEM are internalized by the cells as efficiently as the natural exosomes.

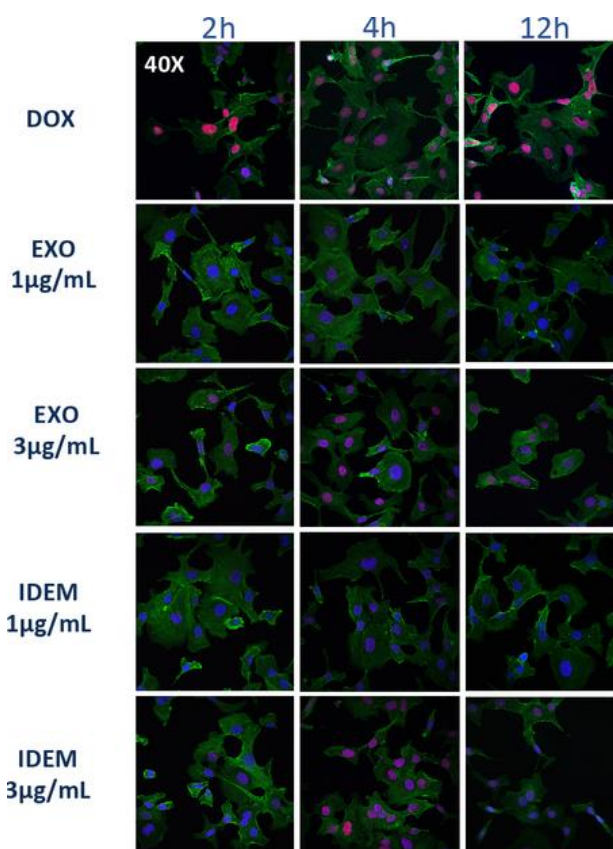


Figure 5.7.1: Confocal microscopy photos et x40 magnification at the three timepoints (2h-4h-12h) of DOX, EXO at the two doses, IDEM at 1 $\mu$ g/mL 3 $\mu$ g/mL.

### 5.7.2. Flow cytometry

Flow cytometry for cellular uptake study was set for one dose only, 3 $\mu$ g/mL, for both nanoparticles and the results obtained confirmed those observed by confocal microscopy. As plotted in **Figure 5.7.2 A**, SKOV3 treated with exosomes (EXO) and the ones treated with IDEM (IDEM) are uptaken by the cells after 2

hours and the fluorescent signal increases overtime, reaching 92.3% for EXO and 94.9% for IDEM after only 2 hours and 99% after 12 hours (**Table 5.7.2**). IDEM are recognized and internalized by the cells. The median fluorescence intensity (MFI, **Figure 5.7.2.B**) allowed to compare the doxorubicin signal released by cells as means of incorporation of EXO and IDEM. The latter shows higher MFI compared to EXO in all the time points considered, meaning that IDEM are more prone to be uptaken by the cells compared to exosomes. Finally, **Figure 5.7.2.1** displays the uptake of different samples divided for the three time-points. The graphs show a higher positive signal to doxorubicin (purple peak) compared to cells alone (green peak). EXO (red) and IDEM (blue) peaks are overlapped in all the timepoints.

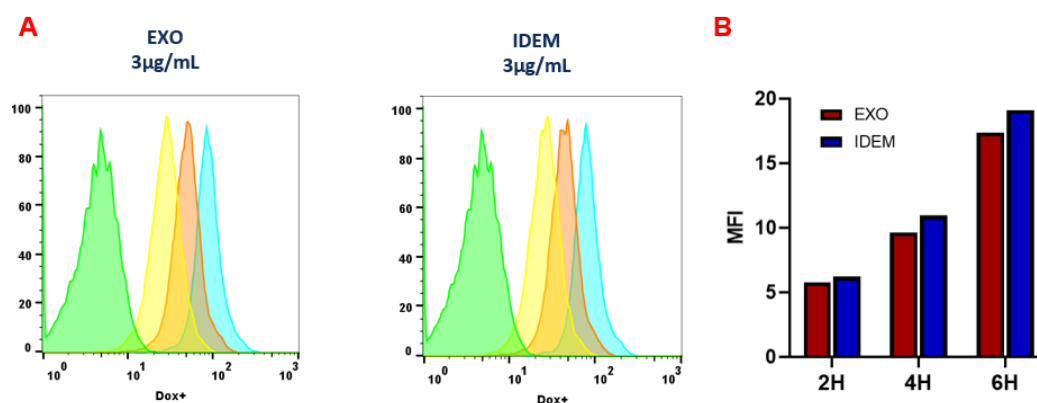


Figure 5.7.2: A) histogram of SKOV3 treated with exosomes (EXO) and with IDEM (IDEM) at 3µg/mL. The legend of the colors is shown in table 3.7. IDEM are uptaken by the cells after 2 hours and the incorporation increases during the monitoring time, so IDEM are recognized by the cells B) Median Fluorescence Intensity (MFI) of doxorubicin signal of EXO and IDEM.

| Sample name | Statistic (%) | Sample name | Statistic (%) |
|-------------|---------------|-------------|---------------|
| CTRL        | 0.9           | CTRL        | 0.99          |
| EXO 2H      | 92.3          | IDEM 2H     | 94.9          |
| EXO 4H      | 98.6          | IDEM 4H     | 99.1          |
| EXO 12H     | 99            | IDEM 12H    | 99.3          |

Table 5.7.2: percentage of positive signal to doxorubicin normalized to control. The incorporation of doxorubicin by the cells with IDEM is around 95% after only 2 hours from the injection

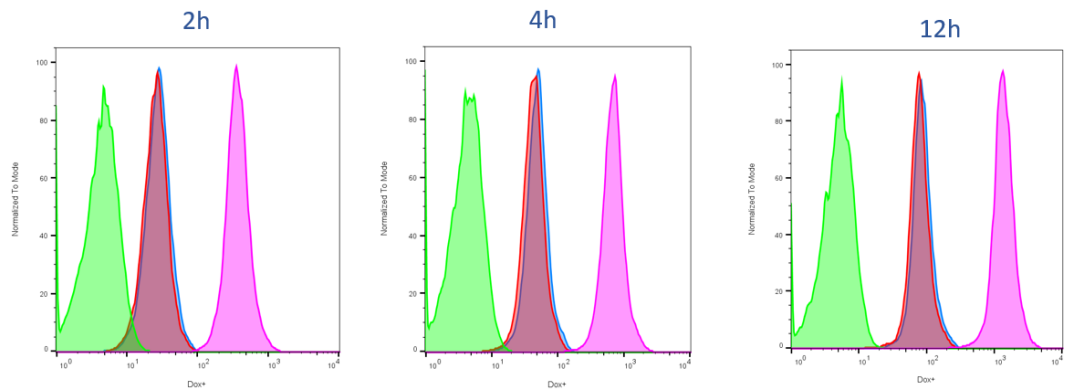


Figure 5.7.2.1: Uptake of doxorubicin of cells treated with EXO and IDEM at  $3\mu\text{g/mL}$  divided for the three time-points. The graphs show a higher positivity to doxorubicin (in purple) compared to the control (in green), but EXO (red) and IDEM (blue) graphs are overlapped overtime.

## 5.8. 3D cultures and IDEM cytotoxicity

The experiment on spheroids is a pilot study that potentially will link 2D experiments with the *in vivo* ones. To understand cell viability in 3D, two parallel aspects were analyzed: average diameter of spheroids, ATP content with fluorescent dye. In **Figure 5.8 a**, photos of spheroids at different time points and with different treatment (a) and the graph of average diameter in function of the different timepoints (b) are shown. **Figure 3.8 b** shows that i) empty particles does not affect negatively spheroid diameter (from 375nm at time 0h to 335nm at 96h), ii) spheroids treated with dox-loaded IDEM determine a 15.5% decrease in diameter, iii) an increase in diameter in spheroids treated with dox-loaded exosomes is registered. However, **Figure 5.8 a** shows that spheroids treated with EXO+DOX are darker, meaning that they are undergoing a necrotic process. We can conclude that spheroid diameter is not a reliable factor of cell viability. In **Figure 5.8.2** the cell viability normalized to control (derived from quantification of ATP content with CellTitrer Glo assay) in function of the different timepoints is shown. It is evident that both controls are not toxic for spheroids, whereas both dox-loaded exosomes and IDEM induce cell death to a greater extent than doxorubicin and as much as doxorubicin, respectively. We can deduce that although IDEM are incorporated in cells, in spheroids, they are cytotoxic only if when dox-loaded.

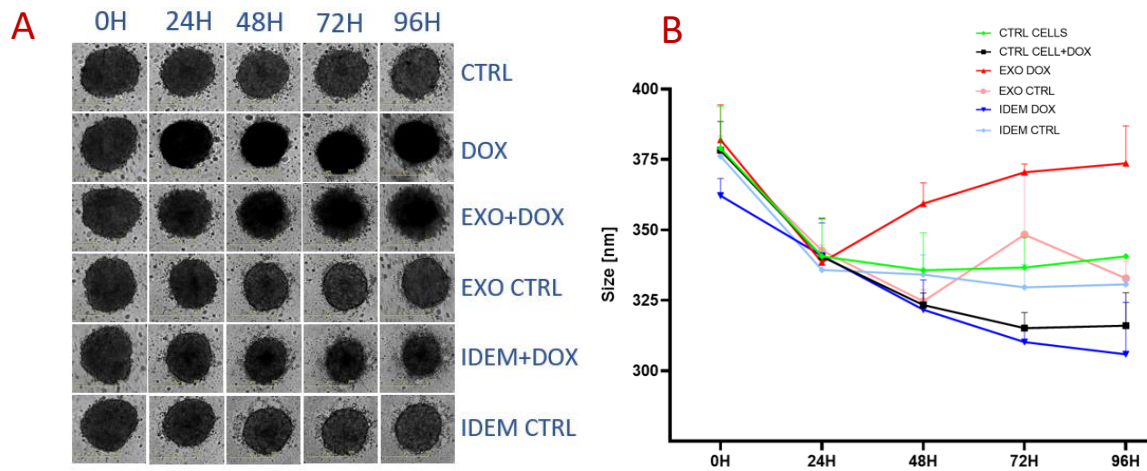


Figure 5.8: Diameter study of spheroids. A) photos of spheroids with different treatments (CTRL, DOX, EXO+DOX, EXO CTRL, IDEM+DOX, IDEM CTRL) at different timepoints (0-24-48-72-96 hours). Necrosis is present in all the spheroids treated with dox-loaded nanoparticles and DOX after 48 hours. A decrease in diameter is evident in IDEM-DOX samples. B) Graph of average spheroid diameter overtime. The EXO-DOX sample show a diameter increase.

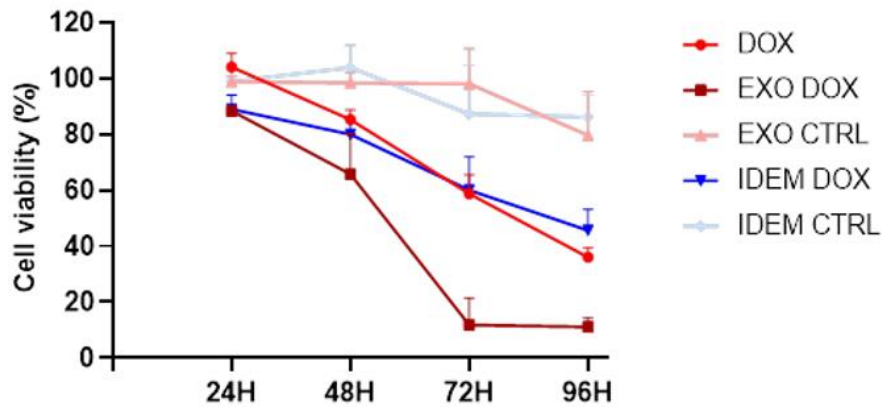


Figure 5.8.2: Percentage of cell viability normalized to control (cells without any treatment) of all the different treatments for 96 hours from CellTiter Glo viability assay. Both controls are not toxic for spheroids, whereas both dox-loaded exosomes and IDEM induce cell death more than doxorubicin and as much as doxorubicin, respectively. We can deduce that IDEM are incorporated in cells in spheroids, but they are cytotoxic only if dox-loaded.

## 6. Conclusions

The aim of the thesis was to develop a strategy to obtain a versatile and smart nanoparticle platform bioinspired by exosomes with the potential to be used as carriers of chemotherapeutics for cancer treatment. The nanoparticles, called IDEM were synthesized and characterized, then loaded with a chemotherapeutic drug and administered to ovarian cancer cells to study their cytotoxic potential. Throughout the entire study, natural exosomes were compared to IDEM in order to assess any differences or advantages when employing the semi-synthetic approach.

As shown by NTA and SEM analysis, it is possible to conclude that through the protocol we optimized for the production of IDEM, a higher yield of exosome mimetics can be obtained. These particles maintain the shape, the dimensions and the size distribution profile of natural exosomes. Furthermore, protein analysis clearly demonstrates that IDEM also express exosomal markers and the same moieties. Doxorubicin-loading of the IDEM and EXO showed that IDEM represent the ideal platform to achieve a greater encapsulation efficiency of drugs compared to exosomes. However, whereas the drug release presents a burst release for the first 6 hours of a percentage of drug higher than 50% for both the nanoparticles, IDEM show more retention of the drug overtime.

Cellular uptake of doxo-loaded exosomes and IDEM by ovarian cancer cells was remarkable soon after the administration of the treatment, with the consequent cytotoxic effect demonstrated in both 2D and 3D culture systems, even at low doses. Finally, from this study we can conclude that IDEM can overcome the limits of exosomes but maintain the biological and physical characteristics of natural exosomes since they are closely comparable in these aspects.

As future perspectives of IDEM, there are development of IDEM loaded with different type of drugs, for different tumor treatments. In this study, the monocytic cell line ThP1 was used as a proof of concept. However, IDEM can be produced starting from different cell types depending on the different cancer therapeutics to be loaded, inherent targeting properties of the parental cells, and the application envisioned.

As future perspectives of IDEM, there are development of IDEM loaded with different type of drugs, for different tumor treatments, from different cell source for different cancer therapeutics. In order to have a complete study of exosomes, it will be also interesting to have a mathematical model of the behavior of exosomes *in vivo*.

## 7. Other skills acquired during the experience at Corradetti Lab

Working at Corradetti Lab allowed me to fully study the exosomes and to express my potentialities in many aspects, from practical laboratory procedures in tissue culture room with the engineering of IDEM, to animal testing of exosomes used as vaccines against ovarian cancer. I had the opportunity to test my communicative skills as I participated in a 3-minutes-speech competition organized by MAPTA (Methodist Association for Postdoctoral and Trainee Affairs) and to improve my capability of rendering and 3D printing for the development of exosome prototypes. This helped me a lot to not be focused on only one aspect of the research, but also to have a deep and complete view of what the mission of Corradetti Lab is.

### 7.1. Animal testing

One of the researches that Corradetti Lab is pursuing is the one that uses exosomes derived from dendritic cells (Dex) as a vaccine for ovarian cancer treatment. By using Dex, it would be possible to both induce the immunoresponse against cancer initiation and progression. For this reason, *in vivo* studies were performed, and I had the opportunity to take part in some of the steps of the experiment that the PhD Student Simone Pisano conceived and developed. Also, I had the opportunity to follow a training on animal experiments provided by the Houston Methodist Research Institute and I could understand another potential interesting application of exosomes in cancer treatment.

First of all, ID8 ovarian cancer cells were injected intraperitoneally in female black mice to produce advanced metastatic cancer; subsequently, the tumor growth was monitored in order to inject the treatment with Dex as soon as the intraperitoneal cavity was colonized by metastases. Chemotherapeutics and PBS were injected mouse-tail-intravenously. The monitoring and imaging of mice was possible thanks to

the machine Spectrum In Vivo Imaging System (IVIS, **Figure 7.1 a** [78]) which combines 2D optical and fluorescent analysis. The system uses optical technology for non-invasive imaging in order to follow up tumor progression and treatment efficacy without sacrificing the mice. The machine can image 5 mice per time, it inhales anesthetics and it heats the imaging platform in order to not stress the mice, it can detect multiples fluorescent signals (430-850nm) with high resolution (20 $\mu$ m) and the new version of the machine can also do parallel 3D Computed Tomography [78]. In this survival study, mice were monitored every 6-7 days and at every detection, they were anesthetized, their abdomen was epilated in order to avoid luminous signal coverage and noise, then they were intraperitoneally injected with luciferin to emit a detectable luminescent signal. The progression of the tumor in mice treated with different nanoparticles were followed up until natural death of the mice. In **Figure 7.1 b** an example of image obtained is shown.

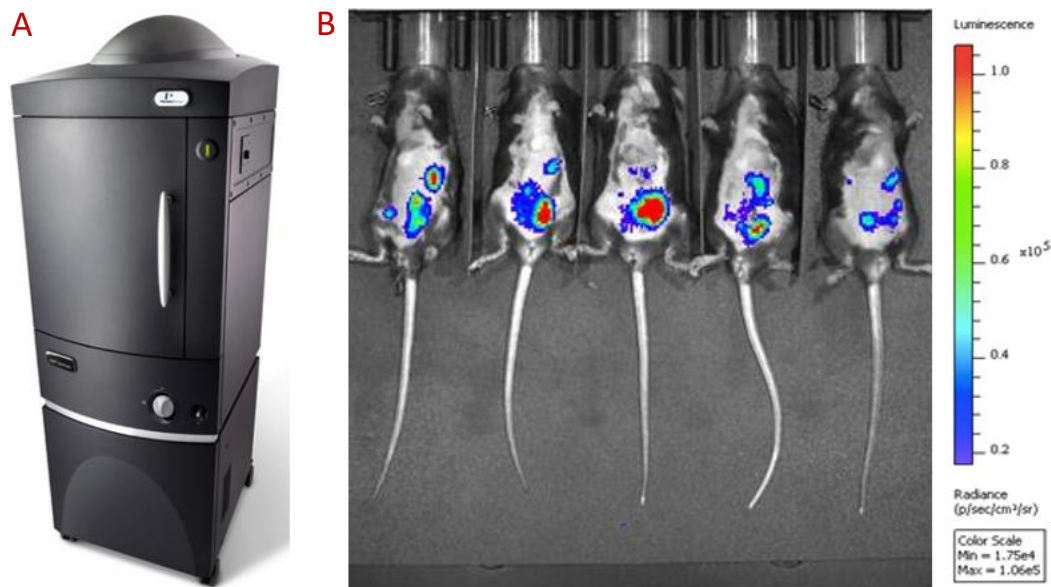


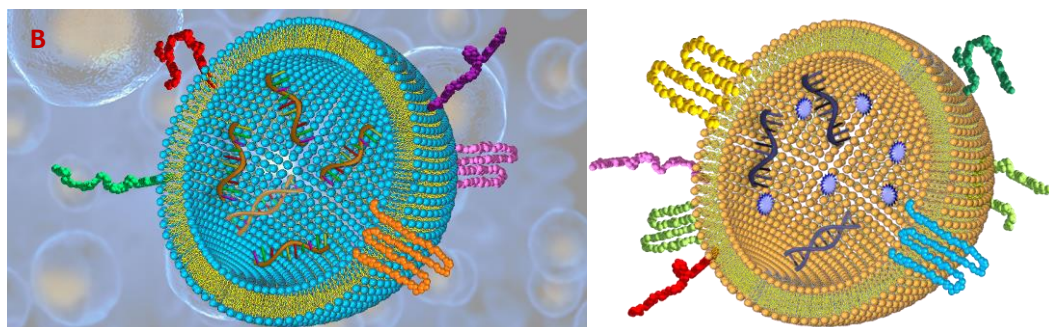
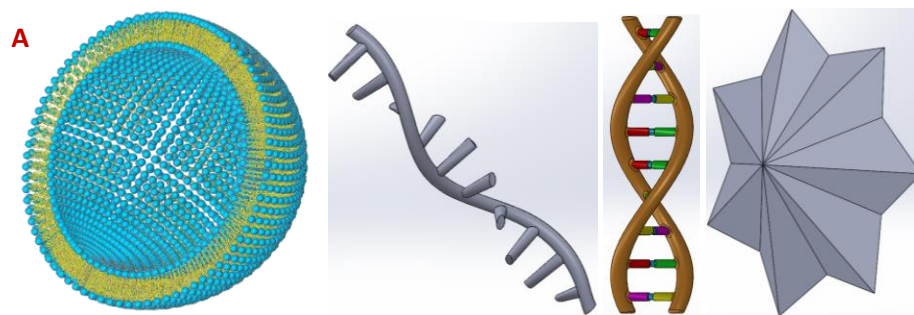
*Figure 7.1: in vivo imaging with IVIS. A) IVIS machine. The mice are placed in the machine while anesthetized and with an injection of luciferin in order to have imaging. Before every measurement, mice were epilated in the abdominal area to allow the signal to be visible and detectable to the machine. B) example of image derived from IVIS analysis. In the image we can see five mice with a tumor in them. The color of the halo is directly related to the luminescence of the tumor in that area, which gives information of the growth of the tumor.*

## 7.2. Rendering of exosomes and 3D printing

To make a scientific message or article more effective and clearer to readers, it is fundamental to have also clear images. This is why part of my experience at Corradetti Lab included rendering and 3D modelling and 3D printing of an exosome. In **Figure 7.2 a**, the different parts of the 3D model are shown, from left to right an exosome, RNA, DNA and a symbolic structure of a drug. For 3D modelling, Solidworks CAD CAM software was employed.

In **Figure 7.2 b** the final rendering of the exosome is shown for two different purposes. For rendering, Solidworks, Photoshop, Power Point (Office 2012) and Biorender were used.

Finally, **Figure 7.2 c** traces all the main steps of 3D modelling, printing and painting of a 3D exosome. For the 3D printer, the “Makerbot Replicator MINI+ 3D printer” from Grattoni Lab (Department of Nanomedicine HMRI) that works with “Makerbot Print 4.7” Software and that ejects PLA polymer was used.



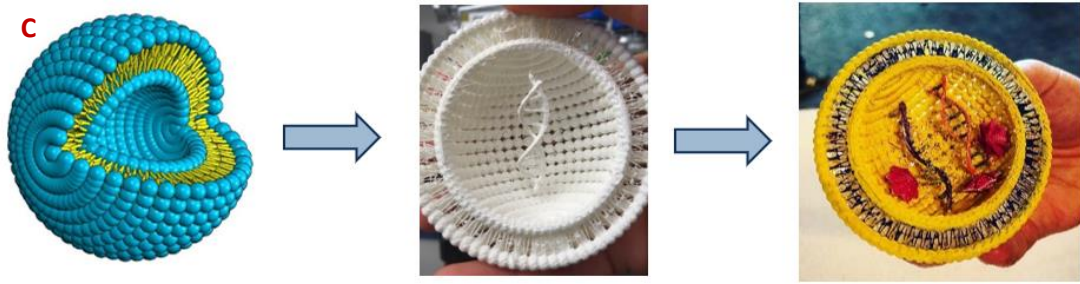


Figure 7.2: 3D printing and rendering of an exosome. A) Different parts of the 3D model, from left to right an exosome, RNA, DNA and a drug. B) final rendering of an exosome. C) Main steps of 3D modelling, printing and painting of a 3D exosome.

## 8. Acknowledgements

Usually this part is the last to be written in a thesis, but I decided that it has to be the first one, because the best way to write a work that concludes five years of my life is by thinking of all the people that I met and loved, to the beautiful and strenuous experiences that I faced, to the emotions that I felt, to the Irene that I was and to the one I am now. In these last years, the first enemy that I fight (and I'm still fighting) is myself: I often was the first person who not believed in me, the first who was complaining during exam sessions and everyday difficulties, the first that sees herself as inferior, stupid, not good enough for anything or beautiful. But I also was, and I am now, the one who accepts all the challenges, all the changes, that loves new experiences, new friends, new air, new books and music, new passions, new knowledges.

So regardless the bad decisions that I may be made, regardless my asper temper that makes everything more spicy, the first person that I have to thank is me: the one that still continues to be strong, curious, explorer, passionate, determinate, keen, funny, bizarre, out of the box and artistic, but also the one that cries, that is angry, stubborn, countercurrent, irascible, that desponds. I've learned a lot from you, Irene, particularly in the last three years, I knew that loneliness is a good and bad friend, I've learned that your times has to be respected, that you need relationships to feel completely alive, that you need your own space for self-expression, that you need to walk instead of running and losing yourself. In these years, everywhere I traveled and studied, I was lucky to have found special people, I built my families and they were fundamental to make my days so unique and the study less hard.

First of all, THANKS to the families I found in Turin: the PELL-RAM + INTRUSI, the ZII, the classmates and Susy and Paolo, my two opera singing teachers.

The PELL-RAM group is with me since the first day of my new life in Turin: even though we had totally different pathways at university, we still know our common origin, the one of the first semesters!! So, thank you Malsha, Vero, Nadia, Gab, Davide, Teo, Brusa, Paolo, Mattia (and obviously Prini) for being so authentic.

The ZII are really my second family, since the first time I met you all I knew that there was something strong between us: the bad smell. We don't need anything complicated to cultivate our friendship, we are dumb and irreverent in the same way and this is absolute perfection! Thanks, from the deep of my heart, to Zio Walter, Zio Luca (first the draft, then the nice copy), the sweet Marta and the plump Sanna. You all are one of the reasons why I'm overjoyed to be back in Turin (if coronavirus will let me it...).

Thanks to Carolina, Eliana, Cristina, Eleonora and Ileana: even though you are the latest university friends that I met, we shared all the tragedies and drama of the last exams! Thank you all for the reciprocal support, study sessions, delirium, spritz and alpacas that we shared.

Thanks to all the enormous and crazy Erasmus crew of Compiègne Automne 2018, in particular Miriam, Angelica, Ilaria and Margherita for being a very powerful quartet! Thanks also to Sandra for keeping our friendship alive and strong even 9000 km far away.

A special thanks goes to Marcella, the one that listens to my interior scream, a sensitive person that helps me the most with the partnership with myself. Her help, empathy and professionalism were fundamental for increasing knowledge on myself and on my life. I also want to thank Susy and Paolo, my opera singing teachers and artistic coaches, the ones that grows my voice and my personality with patience, hard work, criticism and perseverance.

Thanks to my two Houstonian families for being my second home, literally, and for being companion in the semester in Houston: thanks to you all I could learn many things, laugh, explore new cities and be happy, regardless our differences. Thanks to you the thesis was not a boulder, but a shared experience (and remember: puertas se abren a la izquierda!)

Thanks to the “old but gold” friends, the ones that I want to see whenever I come back to my hometown, Ancona: Alice, Alessia, Ilaria, Giada, Priscilla and Marta. You are the prove that long distance friendship can last, even if we see each other three times per year (in the BEST case)!

Enormous thanks goes to the little but powerful Corradetti Lab: my supervisor Bruna Corradetti and the PhD student Simone Pisano. Thank you, Bruna, for being my life coach before being my supervisor, to make me grow up. Thank you for your time, your trust in me, your words, your strength, your independence, your sensitivity, your intelligence and your reproaches. Thank you, Simone for your time, your patience, your knowledges, thanks for being a duo in this semester, regardless all the issues that we had during research, all the incomprehension: we worked a lot together while we gossiped (a lot!), we tried our best in our working and life projects.

Thanks to Polytechnic of Turin, Université de Technologie de Compiègne and Houston Methodist Research Institute, the institutions that grew me during these five years. You were hard teachers, thanks for all the lessons, for all the challenges and opportunities.

Last but not least, I want to thank the real love, the one that never leaved me in all my travels even though I'm always so far or I couldn't feel it: my family, the αγάπη.

Thank you. Grazie.

You gave me the background that I needed to make my decisions, to create my own life, to fly high, but also to know when it's time to come back home and be all together again. Thanks, pone, for being my fluffy teddy bear, to be always so pure and a good listener, to be both funny and reflective at the same time, thank you for all the long talks about everything, they are oxygen for my soul. Thanks, mamma, for being the daily example of a strong, self-made and determinate person, to be so precise, methodic, direct, thanks to make me angry and scrappy, to be a silent helper. Regardless all the fights, misunderstandings, difficult moments that we had, I could not have asked better supporter in my life. Thanks, nonna Irma and nonna Rosa, for being (have been) two

strong women: my heart is full of your tenderness, your resiliency, your simplicity and I'll never forget every single precious moment spent with you two.

Thank you, Mari, for being Mari. I was not forgetting you! You are the most important person in my life. Thank you for being my big sister with a big heart, this is the essential. Thank you for make me feel perfect, thank you for being perfection. This work is for you.

## 9. Bibliography

- [1] National Institutes of Health (US); Biological Sciences Curriculum Study. NIH Curriculum Supplement Series [Internet]. Bethesda (MD): National Institutes of Health (US); 2007. Understanding Cancer. Available from: <https://www.ncbi.nlm.nih.gov/books/NBK20362/>
- [2] Saxena, Meera & Christofori, Gerhard. (2013). Rebuilding cancer metastasis in the mouse. *Molecular oncology*. 7. 10.1016/j.molonc.2013.02.009.
- [3] WEBMD MEDICAL REFERENCE; [www.webMD.com](http://www.webMD.com); [online]; Nayana Ambardekar; July 30<sup>th</sup> 2019; viewed on March 12<sup>th</sup> 2020; <https://www.webmd.com/a-to-z-guides/benign-tumors-causes-treatments#1>
- [4] ANNE LODGE; [www.astartebio.com](http://www.astartebio.com); [online]; Bothell, WA; August 1<sup>st</sup> 2019; viewed on March 15<sup>th</sup> 2020; <https://astartebio.com/blog/immunology-for-non-immunologists-hot-vs-cold-tumors/>
- [5] WEBMD MEDICAL REFERENCE; [www.webMD.com](http://www.webMD.com); [ONLINE]; NIH National Cancer Institute: "Radiation Therapy for Cancer," "Biological Therapies for Cancer," "Chemotherapy and You: Support for People With Cancer." National Cancer Society: "What Is Targeted Cancer Therapy?" OncoLink.org: "Intraperitoneal Chemotherapy (IP Chemo)."; Gabriela Pichardo; January 26<sup>th</sup> 2020; viewed on March 17<sup>th</sup> 2020; <https://www.webmd.com/cancer/chemotherapy-what-to-expect#1>
- [6] Saxena, Meera & Christofori, Gerhard. (2013). Rebuilding cancer metastasis in the mouse. *Molecular oncology*. 7. 10.1016/j.molonc.2013.02.009.
- [7] NATIONAL INSITUTE OF HEALTH (NIH); [www.cancer.gov](http://www.cancer.gov); [online]; viewed on March 15<sup>th</sup> 2020; <https://www.cancer.gov/about-cancer/treatment/types>
- [8] Greish K. (2010) Enhanced Permeability and Retention (EPR) Effect for Anticancer Nanomedicine Drug Targeting. In: Grobmyer S., Moudgil B. (eds) *Cancer Nanotechnology. Methods in Molecular Biology (Methods and Protocols)*, vol 624. Humana Press

- [9] Albinali KE, Zagho MM, Deng Y, Elzatahry AA. A perspective on magnetic core–shell carriers for responsive and targeted drug delivery systems. *Int J Nanomedicine*. 2019;14:1707-1723  
<https://doi.org/10.2147/IJN.S193981>
- [10] Johnstone RM, Adam M, Hammond JR, Orr L, Turbide C. Vesicle formation during reticulocyte maturation. Association of plasma membrane activities with released vesicles (exosomes) *J Biol Chem*. 1987;262(19):9412–9420.
- [11] Costanza Emanuelli, Andrew I.U. Shearn, Gianni D. Angelini, Susmita Sahoo, Exosomes and exosomal miRNAs in cardiovascular protection and repair, *Vascular Pharmacology*, Volume 71, 2015, ISSN 1537-1891, <https://doi.org/10.1016/j.vph.2015.02.008>.  
(<http://www.sciencedirect.com/science/article/pii/S153718911500049X>)
- [12] Minciacchi VR, Freeman MR, Di Vizio D. Extracellular vesicles in cancer: exosomes, microvesicles and the emerging role of large oncosomes. *Semin Cell Dev Biol*. 2015;40:41–51. doi: 10.1016/j.semcdb.2015.02.010
- [13] Huang T, Deng CX. Current Progresses of Exosomes as Cancer Diagnostic and Prognostic Biomarkers. *Int J Biol Sci*. 2019;15(1):1–11. Published 2019 Jan 6. doi:10.7150/ijbs.27796
- [14] Maia J, Caja S, Strano Moraes MC, Couto N and Costa-Silva B (2018) Exosome-Based Cell-Cell Communication in the Tumor Microenvironment. *Front. Cell Dev. Biol.* 6:18. doi: 10.3389/fcell.2018.00018
- [15] UNIVERSITY OF CALCUTTA; [www.slideshare.net](http://www.slideshare.net); [ONLINE]; viewed on March 17<sup>th</sup> 2020; <https://www.slideshare.net/DebanjanChatterjee13/physiological-barriers-by-debanjan-chatterjee-abhishek-roy>
- [16] Ill-Min Chung, Govindasamy Rajakumar, Baskar Venkidasamy, Umadevi Subramanian, Muthu Thiruvengadam, Exosomes: Current use and future applications, *Clinica Chimica Acta*, Volume 500, 2020, Pages 226-232, ISSN 0009-8981, <https://doi.org/10.1016/j.cca.2019.10.022>.  
(<http://www.sciencedirect.com/science/article/pii/S0009898119320881>)

- [17] Yuan MJ, Maghsoudi T, Wang T. Exosomes Mediate the Intercellular Communication after Myocardial Infarction. *Int J Med Sci* 2016; 13(2):113-116. doi:10.7150/ijms.14112. Available from <http://www.medsci.org/v13p0113.htm>
- [18] Han, C., Sun, X., Liu, L., Jiang, H., Shen, Y., Xu, X., ... Wang, T. (2016). *Exosomes and Their Therapeutic Potentials of Stem Cells. Stem Cells International, 2016, 1–11.* doi:10.1155/2016/7653489
- [19] Skog J, Würdinger T, van Rijn S, Meijer DH, Gainche L, Curry WT, et al. Glioblastoma microvesicles transport RNA and proteins that promote tumour growth and provide diagnostic biomarkers. *Nat Cell Biol.* 2008;10:1470-6. 10.1038/ncb1800
- [20] Hong B, Cho JH, Kim H, Choi EJ, Rho S, Kim J, et al. Colorectal cancer cell-derived microvesicles are enriched in cell cycle-related mRNAs that promote proliferation of endothelial cells. *BMC Genomics.* 2009;10:556. 10.1186/1471-2164-10-556
- [21] Tai YL, Chen KC, Hsieh JT, Shen TL. Exosomes in cancer development and clinical applications. *Cancer Sci.* 2018;109(8):2364–2374. doi:10.1111/cas.13697
- [22] Sugiyama, Toru & Kumagai, Seisuke. (2009). Pegylated Liposomal Doxorubicin for Advanced Ovarian Cancer in Women who are Refractory to Both Platinum- and Paclitaxel-Based Chemotherapy Regimens. *Clinical Medicine. Therapeutics.* 1. CMT.S2219. 10.4137/CMT.S2219.
- [23] Desai N. (2016) Nanoparticle Albumin-Bound Paclitaxel (Abraxane®). In: Otagiri M., Chuang V. (eds) *Albumin in Medicine.* Springer, Singapore
- [24] Falagan-Lotsch, P., Grzincic, E.M., & Murphy, C.J. (2017). New Advances in Nanotechnology-Based Diagnosis and Therapeutics for Breast Cancer: An Assessment of Active-Targeting Inorganic Nanoplatfoms. *Bioconjugate chemistry,* 28 1, 135-152.
- [25] Couvreur, P. (2013). Nanoparticles in drug delivery: Past, present and future. *Advanced Drug Delivery Reviews,* 65(1), 21–23. doi:10.1016/j.addr.2012.04.010

- [26] Patel, G.K., Khan, M.A., Zubair, H. *et al.* Comparative analysis of exosome isolation methods using culture supernatant for optimum yield, purity and downstream applications. *Sci Rep* **9**, 5335 (2019). <https://doi.org/10.1038/s41598-019-41800-2>
- [27] Goh, W.J., Zou, S., Ong, W.Y. *et al.* Bioinspired Cell-Derived Nanovesicles *versus* Exosomes as Drug Delivery Systems: a Cost-Effective Alternative. *Sci Rep* **7**, 14322 (2017). <https://doi.org/10.1038/s41598-017-14725-x>
- [28] Tang, Y., Huang, Y., Zheng, L., Qin, S., Xu, X., An, T. ... Wang, Q. (2017). Comparison of isolation methods of exosomes and exosomal RNA from cell culture medium and serum. *International Journal of Molecular Medicine*, **40**, 834-844. <https://doi.org/10.3892/ijmm.2017.3080>
- [29] Franquesa M, Hoogduijn MJ, Ripoll E, et al. Update on controls for isolation and quantification methodology of extracellular vesicles derived from adipose tissue mesenchymal stem cells. *Front Immunol.* 2014;5:525. Published 2014 Oct 21. doi:10.3389/fimmu.2014.00525
- [30] Smith JA, Leonardi T, Huang B, Iraci N, Vega B, Pluchino S. Extracellular vesicles and their synthetic analogues in aging and age-associated brain diseases. *Biogerontology.* 2015;16(2):147–185. doi:10.1007/s10522-014-9510-7
- [31] Li X, Corbett AL, Taatizadeh E, et al. Challenges and opportunities in exosome research- Perspectives from biology, engineering, and cancer therapy. *APL Bioeng.* 2019;3(1):011503. Published 2019 Mar 27. doi:10.1063/1.5087122
- [32] Momen-Heravi F, Balaj L, Alian S, et al. Current methods for the isolation of extracellular vesicles. *Biol Chem.* 2013;394(10):1253–1262. doi:10.1515/hsz-2013-0141
- [33] Exosomes: Isolation and Characterization Methods and Specific Markers, Konstantin Yakimchuk (Konstantin dot Yakimchuk at ki dot se) Karolinska Institutet, Stockholm, Sweden DOI//dx.doi.org/10.13070/mm.en.5.1450 original version : 2015-08-15
- [34] Li, S., Lin, Z., Jiang, X. *et al.* Exosomal cargo-loading and synthetic exosome-mimics as potential therapeutic tools. *Acta Pharmacol Sin* **39**, 542–551 (2018). <https://doi.org/10.1038/aps.2017.178>

[35] AGENZIA ZOE, informazione medico-scientifica; [www.airc.it](http://www.airc.it); [online]; Milano; Fondazione AIRC per la ricerca sul cancro; April 24th 2017; viewed on March 15th 2020; <https://www.airc.it/cancro/informazioni-tumori/guida-ai-tumori/tumore-delle-ovaie>

[36] Reid BM, Permuth JB, Sellers TA. Epidemiology of ovarian cancer: a review. *Cancer Biol Med.* 2017;14(1):9–32. doi:10.20892/j.issn.2095-3941.2016.0084

[37] VIVERE PIU SANI; [www.viverepiusani.it](http://www.viverepiusani.it); [ONLINE]; October 12th 2018; viewed on March 15<sup>th</sup> 2020; <https://viverepiusani.it/segni-cancro-dellovaio-non-ignorare/>

[38] Li, X., Wang, X. The emerging roles and therapeutic potential of exosomes in epithelial ovarian cancer. *Mol Cancer* **16**, 92 (2017). <https://doi.org/10.1186/s12943-017-0659-y>

[39] Gao D, Jiang L. Exosomes in cancer therapy: a novel experimental strategy. *Am J Cancer Res.* 2018;8(11):2165–2175. Published 2018 Nov 1.

[40] Brennetta J. Crenshaw, Brian Sims and Qiana L. Matthews (November 5th 2018). Biological Function of Exosomes as Diagnostic Markers and Therapeutic Delivery Vehicles in Carcinogenesis and Infectious Diseases, Nanomedicines, Muhammad Akhyar Farrukh, IntechOpen, DOI: 10.5772/intechopen.80225. <https://www.intechopen.com/books/nanomedicines/biological-function-of-exosomes-as-diagnostic-markers-and-therapeutic-delivery-vehicles-in-carcinoge>

[41] “Bioinspired Exosome-Mimetic Nanovesicles for Targeted Delivery of Chemotherapeutics to Malignant Tumors. Jang, S. C., Kim, O. Y., Yoon, C. M., Choi, D.-S., Roh, T.-Y., Park, J., Gho, Y. S. (2013)”

[42] Filipe V, Hawe A, Jiskoot W. Critical evaluation of Nanoparticle Tracking Analysis (NTA) by NanoSight for the measurement of nanoparticles and protein aggregates. *Pharm Res.* 2010;27(5):796–810. doi:10.1007/s11095-010-0073-2

[43] ASTM E2834-12, Standard Guide for Measurement of Particle Size Distribution of Nanomaterials in Suspension by Nanoparticle Tracking Analysis (NTA), ASTM International, West Conshohocken, PA, 2012, [www.astm.org](http://www.astm.org); <https://www.particle>

[metrix.de/en/technologies/nanoparticle-tracking/articles-nanoparticle-tracking/introduction-to-nanoparticle-tracking-analysis-nta](https://metrix.de/en/technologies/nanoparticle-tracking/articles-nanoparticle-tracking/introduction-to-nanoparticle-tracking-analysis-nta)

[44] ANDREW MALLOY; [www.genengnews.com](http://www.genengnews.com); [ONLINE]; Genetic Engineering & Biotechnology News; last update on April 1<sup>st</sup> 2012; viewed on March 5<sup>th</sup> 2020; <https://www.genengnews.com/magazine/179/exosome-and-microvesicle-characterization/#>

[45] ISBG, ENABLING TECHNOLOGIES FOR THE FRENCH AND EUROPEAN STRUCTURAL BIOLOGY COMMUNITY, CAROLINE MAS, DENIS MÉYÈER AURIANE; [www.isbg.fr](http://www.isbg.fr); [ONLINE]; August 2<sup>nd</sup> 2019; viewed on March 5<sup>th</sup> 2020; <https://www.isbg.fr/biophysics-characterisation/nanoparticle-tracking-analysis-nta/?lang=fr>

[46] Inkson, B. J. (2016). Scanning electron microscopy (SEM) and transmission electron microscopy (TEM) for materials characterization. Materials Characterization Using Nondestructive Evaluation (NDE) Methods, 17–43. doi:10.1016/b978-0-08-100040-3.00002-x

[47] ALFATEST STRUMENTAZIONE SCIENTIFICA; [www.alfatest.it](http://www.alfatest.it); [ONLINE]; Roma; viewed on March 8<sup>th</sup> 2020; <https://www.alfatest.it/tecniche/sem-microscopia-elettronica-scansione>

[48] BIOLEGEND INC.; [www.biolegend.com](http://www.biolegend.com); [ONLINE]; San Diego, CA; 2020; viewed on March 6<sup>th</sup> 2020; <https://www.biolegend.com/en-us/western-blot>

[49] The Protein Man's Blog | A Discussion of Protein Research ELISA Blocking Agents & Blocking Solutions Posted by The Protein Man on Jul 25, 2017 2:30:00 PM <https://info.gbiosciences.com/blog/elisa-blocking-agents-blocking-solutions>

[50] BOSTER BIOLOGICAL TECHNOLOGY; [www.bosterbio.com](http://www.bosterbio.com); [ONLINE]; Pleasanton, CA; viewed on March 6<sup>th</sup> 2020; <https://www.bosterbio.com/protocol-and-troubleshooting/flow-cytometry-principle>

[51] THERMO FISHER SCIENTIFIC; [www.thermofisher.com](http://www.thermofisher.com); [ONLINE]; viewed on March 8<sup>th</sup> 2020; <https://www.thermofisher.com/us/en/home/life-science/cell-analysis/cell-analysis-learningcenter/molecular-probes-school-of-fluorescence/flow-cytometry-basics/flow-cytometryfundamentals/how-flow-cytometer-works.html>

[52] Qian, Yu; Wei, Chungwen; Eun-Hyung Lee, F.; Campbell, John; Halliley, Jessica; Lee, Jamie A.; Cai, Jennifer; Kong, Y. Megan et al. (2010). «Elucidation of seventeen human peripheral blood B-cell subsets and quantification of the tetanus response using a density-based method for the automated identification of cell populations in multidimensional flow cytometry data». *Cytometry Part B: Clinical Cytometry*. 78B: S69.

[53] MIKE KISSNER, CHEEKY SCIENTIST TECHNICAL PROGRAMS; [www.expert.cheekyscientist.com](http://www.expert.cheekyscientist.com); [ONLINE]; Liberty lake, WA; TIM BUSHNELL; viewed on March 4<sup>th</sup> 2020; <https://expert.cheekyscientist.com/whats-flow-cytometry-light-scatter-how-cell-size-particle-size-affects-it/>

[54] Van Dilla, M.A., Dean, P.N., Laerum, O.D. and Melamed, M.R. (eds.) (1985). *Flow cytometry instrumentation and data analysis*. Academic Press, Orlando. CREATIVE DIAGNOSTICS; [www.creative-diagnostics.com](http://www.creative-diagnostics.com); [ONLINE]; <https://www.creative-diagnostics.com/flow-cytometry-guide.htm>

[55] BIO-RAD LABORATORIES; [www.bio-rad-antibodies.com](http://www.bio-rad-antibodies.com); [ONLINE]; 2020; viewed on March 7<sup>th</sup> 2020; <https://www.bio-rad-antibodies.com/alarblue-cell-viability-assay-resazurin.html>

[66] INTERCHIM; [www.interchim.fr](http://www.interchim.fr); [ONLINE]; Montlucon Cedex, France; viewed on March 7<sup>th</sup> 2020; <https://www.interchim.fr/ft/6/66941f.pdf>

[57] Time-dependent cytotoxic drugs selectively cooperate with IL-18 for cancer chemo-immunotherapy Ioannis Alagkiozidis, Andrea Facciabene, Marinos Tsiatas, Carmine Carpenito, Fabian Benencia, Sarah Adams, Zdenka Jonak, Carl H June, Daniel J Powell, Jr, and George Coukos

[58] Acetaminophen Enhances Cisplatin- and Paclitaxel-mediated Cytotoxicity to SKOV3 Human Ovarian Carcinoma ying-jen jeffrey wu, alexander j. neuwelt, leslie l. muldoon and edward a. neuwelt

[59] Cancer stem-like cells can be isolated with drug selection in human ovarian cancer cell line SKOV3. Ma, L., Lai, D., Liu, T., Cheng, W., & Guo, L. (2010). *Acta Biochimica et Biophysica Sinica*, 42(9), 593–602. doi:10.1093/abbs/gmq067

[60] An evaluation of cytotoxicity of the taxane and platinum agents combination treatment in a panel of human ovarian carcinoma cell lines. Smith, J. A., Ngo, H., Martin, M. C., & Wolf, J. K. (2005). *Gynecologic Oncology*, 98(1), 141–145. doi:10.1016/j.ygyno.2005.02.006

[61] Increased immunogenicity of surviving tumor cells enables cooperation between liposomal doxorubicin and IL-18 Ioannis Alagkiozidis, Andrea Facciabene, Carmine Carpenito, Fabian Benencia, Zdenka Jonak Sarah Adams, Richard G Carroll, Phyllis A Gimotty, Rachel Hammond, Gwen-ael Danet-Desnoyers, Carl H June, Daniel J Powell Jr & [...]George Coukos

[62] AGILENT; [www.agilent.com](http://www.agilent.com); [ONLINE] ; Santa Clara, CA; 2020 ; viewed on March 6<sup>th</sup> 2020; <https://www.agilent.com/en/products/cell-analysis/real-time-cell-analyzers/xcelligence-rtca-esight>

[63] Comparative Study of the Sensitivities of Cancer Cells to Doxorubicin, and Relationships between the Effect of the Drug-Efflux Pump P-gp. Kibria, G., Hatakeyama, H., Akiyama, K., Hida, K., & Harashima, H. (2014). *Biological and Pharmaceutical Bulletin*, 37(12), 1926–1935. doi:10.1248/bpb.b14-00529

[64] Goh, W. J., Lee, C. K., Zou, S., Woon, E., Czarny, B., & Pastorin, G. (2017). Doxorubicin-loaded cell-derived nanovesicles: an alternative targeted approach for anti-tumor therapy. *International Journal of Nanomedicine*, Volume 12, 2759–2767. doi:10.2147/ijn.s131786

[65] Shah S, Chandra A, Kaur A, et al. Fluorescence properties of doxorubicin in PBS buffer and PVA films. *J Photochem Photobiol B*. 2017;170:65–69. doi:10.1016/j.jphotobiol.2017.03.024

[66] Liang, Junyu & Zhang, Zhigao & Zhao, Hui & Wan, Shanhe & Zhai, Xiangming & Zhou, Jianwei & Liang, Rongliang & Deng, Qiaoting & Wu, Yingsong & Lin, Guanfeng. (2018). Simple and rapid monitoring of doxorubicin using streptavidin-modified microparticle-based time-resolved fluorescence immunoassay. *RSC Advances*. 8. 15621-15631. 10.1039/C8RA01807C.

[67] Jørgen Fogh, Jens M. Fogh, Thomas Orfeo; One Hundred and Twenty-Seven Cultured Human Tumor Cell Lines Producing Tumors in Nude Mice, *JNCI: Journal of the National Cancer Institute*, Volume 59, Issue 1, 1 July 1977, Pages 221–226, <https://doi.org/10.1093/jnci/59.1.221>

[68] xCELLigence RTCA eSight Biosensor Technology meets live cell imaging, Kenneth Chan, PhD, cell analysis Agilent technologies presentation

[69] AGILENT; Jing Zhang, Nancy Li, Yama Abassi and Brandon J. Lamarche. Agilent Technologies Inc. San Diego, CA, USA. Grace Yang, Jiaming Zhang and Peifang Ye. Agilent Biosciences Co. Ltd. Hangzhou, China. <https://www.agilent.com/cs/library/applications/application-combining-live-cell-imaging-cell-analysis-5994-1212en-agilent.pdf>

[70] Pawley JB (editor) (2006). *Handbook of Biological Confocal Microscopy (3rd ed.)*. Berlin: Springer. <https://www.biofotonica.it/tecnologie/microscopia-confocale/>

[71] DAVE JOHNSTON and ANTON PAGE; [www.cdn.southampton.ac.uk](http://www.cdn.southampton.ac.uk); [ONLINE]; viewed on March 8<sup>th</sup> 2020;

[https://cdn.southampton.ac.uk/assets/imported/transforms/contentblock/UsefulDownloads\\_Download/EAA2CA3E29A845709A8224D05DB9CD40/GroupConfocalWeb.pdf](https://cdn.southampton.ac.uk/assets/imported/transforms/contentblock/UsefulDownloads_Download/EAA2CA3E29A845709A8224D05DB9CD40/GroupConfocalWeb.pdf)

[72]FACULTE DES SCIENCES FONDAMENTALES ET BIOMEDICALES UNIVERSITE PARIS DESCARTES, SCM ; [www.biomedicale.parisdescartes.fr](http://www.biomedicale.parisdescartes.fr); [ONLINE] ; Paris, FR ; viewed on March 8th 2020 ; [http://www.biomedicale.parisdescartes.fr/scm/introduction\\_microscopie\\_confocale.html](http://www.biomedicale.parisdescartes.fr/scm/introduction_microscopie_confocale.html)

[73] Czymmek, Kirk & Dahms, Tanya. (2015). Future Directions in Advanced Mycological Microscopy. 10.1007/978-3-319-22437-4\_8.

[74] Kapałczyńska M, Kolenda T, Przybyła W, et al. 2D and 3D cell cultures - a comparison of different types of cancer cell cultures. *Arch Med Sci*. 2018;14(4):910–919. doi:10.5114/aoms.2016.63743

[75] Nunes, AS, Barros, AS, Costa, EC, Moreira, AF, Correia, IJ. 3D tumor spheroids as *in vitro* models to mimic *in vivo* human solid tumors resistance to therapeutic drugs. *Biotechnology and Bioengineering*. 2018; <https://doi.org/10.1002/bit.26845>

[76] Ishiguro T, Ohata H, Sato A, Yamawaki K, Enomoto T, Okamoto K. Tumor-derived spheroids: Relevance to cancer stem cells and clinical applications. *Cancer Sci.* 2017;108(3):283–289. doi:10.1111/cas.13155

[77] PROMEGA; [www.promega.com](http://www.promega.com); [ONLINE]; Madison, WI; 11/15; viewed on March 8<sup>th</sup> 2020; <https://www.promega.com/-/media/files/resources/protocols/technicalmanuals/101/celltiter-glo-3d-cell-viability-assay-protocol.pdf?la=en>

[78] PERKINELMER; [www.perkinelmer.com](http://www.perkinelmer.com); [ONLINE]; viewed on March 14<sup>th</sup> 2020; <https://www.perkinelmer.com/it/product/ivis-instrument-spectrum-120v-andor-c-124262>